AD-A135 972 EXCITONIC SOLIDS(U) RENSSELAERPOLYTECHNIC INST TROY N Y DIV OF MATRRIALS ENGINEERING R K MACCRONE 03 NOV 83 AFOSR-TR-83-0997 AFOSR-79-0126 1/1

UNCLASSIFIED F/G 20/12 NL

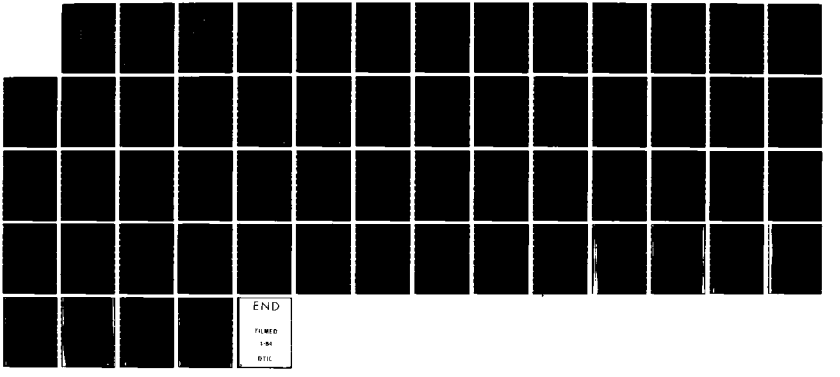

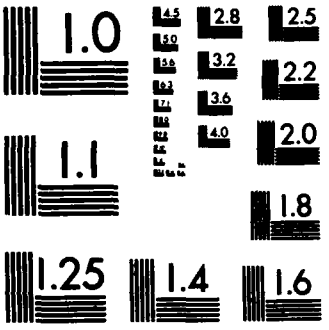

MICROCOPY RESOLUTION TEST CHART
NATIONAL BUREAU OF STANDARDS-1963-A

UNCLASSIFIED

SECURITY CLASSIFICATION OF THIS PAGE *(When Data Entered)*

(12)

REPORT DOCUMENTATION PAGE	READ INSTRUCTIONS BEFORE COMPLETING FORM
1. REPORT NUMBER: AFOSR-TR- 83-0997	2. GOVT ACCESSION NO. AD-A135972 / 3. RECIPIENT'S CATALOG NUMBER
4. TITLE *(and Subtitle)*: EXCITONIC SOLIDS	5. TYPE OF REPORT & PERIOD COVERED: FINAL
	6. PERFORMING ORG. REPORT NUMBER
7. AUTHOR(s): Robert.K. MacCrone	8. CONTRACT OR GRANT NUMBER(s): AFOSR-79-0126
9. PERFORMING ORGANIZATION NAME AND ADDRESS: Rensselaer Polytechnic Institute, Materials Engineering Department, Troy, NY 12181	10. PROGRAM ELEMENT, PROJECT, TASK AREA & WORK UNIT NUMBERS: 2301/A8, 61102F
11. CONTROLLING OFFICE NAME AND ADDRESS: AFOSR/NP, Bolling AFB, Wash DC, 20332	12. REPORT DATE: 3 Nov 83
	13. NUMBER OF PAGES: 56
14. MONITORING AGENCY NAME & ADDRESS*(if different from Controlling Office)*	15. SECURITY CLASS. *(of this report)*: UNCLASSIFIED
	15a. DECLASSIFICATION/DOWNGRADING SCHEDULE

16. DISTRIBUTION STATEMENT *(of this Report)*

Approved for public release; distribution unlimited

17. DISTRIBUTION STATEMENT *(of the abstract entered in Block 20, if different from Report)*

18. SUPPLEMENTARY NOTES

DEC 1 9 1983

A

19. KEY WORDS *(Continue on reverse side if necessary and identify by block number)*

20. ABSTRACT *(Continue on reverse side if necessary and identify by block number)*

The investigators have made experimental measurements of the diamagnetism of CdS and have attempted to understand the anomolous effects by theoretical analysis. These studies have contributed to understanding the contribution of impurities to the anomalous diamagnetism in CdS.

DD FORM 1 JAN 73 1473

UNCLASSIFIED

SECURITY CLASSIFICATION OF THIS PAGE *(When Data Entered)*

DISCLAIMER NOTICE

THIS DOCUMENT IS BEST QUALITY PRACTICABLE. THE COPY FURNISHED TO DTIC CONTAINED A SIGNIFICANT NUMBER OF PAGES WHICH DO NOT REPRODUCE LEGIBLY.

FINAL REPORT

AFOSR Contract No. AFOSR-79-0126

entitled "EXCITONIC SOLIDS"

Robert K. MacCrone
Professor
Materials Engineering Department
Rensselaer Polytechnic Institute
Troy, New York 12181

November 3, 1983

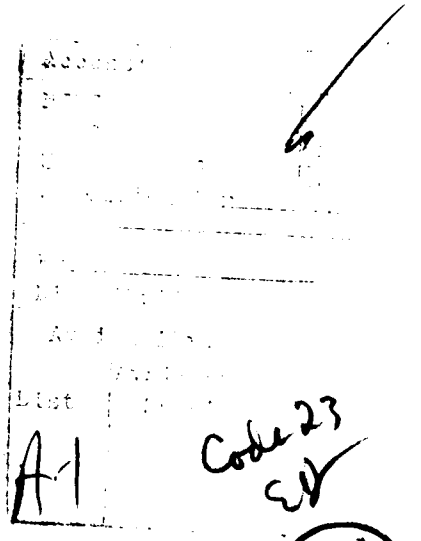

BACKGROUND

Our proposal called for a study of selected physical properties of CdS doped with chlorine of varying concentrations. The motivation for this study was the observation of anomalous magnetic and electrical properties of particular specimens that had been pressure quenched from above the cubic to Wurtzite transition, and to determine the prerequisites in the samples for the effects.

We outlined a program to investigate the optical-band edge dependence and photo-conductivity as a function of chlorine concentration as related to the magnetic effects.

To this end we purchased the photo-acoustic spectrometer as proposed, interfaced the equipment to our optical and computer facilities and proceeded with a systematic study which is described in detail in the next section.

A M.S. student, David Campbell has been supported on the project, and his thesis on the subject is expected in the Summer of 1984. A publication is anticipated.

Other publications of work supported by the grant, and other associated work, are appended.

Finally, we wish to express our gratitude for the financial support of the AFOSR in this matter.

OPTICAL PROPERTIES OF Cl DOPED CdS

INTRODUCTION

Our previous work on Cl doped CdS has shown the existence of large diamagnetism of Meissner proportions at 77K in pressure quenched material.[1] This suggests the possibility of a high temperature superconducting state in the NaCl-Wurtzite phases produced by pressure quenching. Since it is known that the Cl concentration of the material affects the fraction that remains in the NaCl structure after quenching,[2] it is of importance to study the effect of the Cl doping on the electronic state and other properties of the CdS crystal. It has been noted that the incorporation of chlorine or other halide in CdS increases the conductivity and the photosensitivity.[3]

In order to further investigate the effect of heavily doping CdS, optical absorption and photoconductivity in the visible region have been studied for various chlorine concentrations. A shift of the apparent absorption edge and also a shift in the peak photoresponse is evident. Results suggest the formation of an impurity band which narrows the energy gap of the crystal at higher dopant concentrations. The concentration at which the impurity band is first formed is close to the critical concentration required for the diamagnetism.[4]

The photoconductivity of pressure quenched material was also studied and both a change in energy gap and a metastable structure in the material are indicated.

EXPERIMENTAL

Chlorine doped CdS material was received, in powder form from the National Bureau of Standards.[5] The material was precipitated by bubbling H_2S gas through $CdCl_2$ solution. The dopant concentrations of the materials used are given in Table I. Pure CdS powders were obtained from Alpha Inorganic and Eagle Pitcher Companies. The powders were formed into small cylindrical pellets (2.5mm dia.) in a hand press.

In order to study the absorption of the various samples of Cl-doped CdS a photoacoustic spectroscopy system was set up. This allowed absorption measurements to be made on all types of samples (powder, pressed powder, single crystal) with no sample preparation needed.[6] The PAS system consists of a light source, monochromator, light modulator, photoacoustic cell and signal processing components as shown in Fig. 1. The sample cell and pre-amplifier were purchased from Princeton Applied Research Corporation. A PAR 5204 phase sensitive lock-in amplifier was also used. The optical system consisted of a B&L monochromator driven by a low speed synchronous motor, a four-blade rotating chopper and a quartz lens and mirror assembly. Light was provided by either a 1000W Xenon arc or quartz halogen filament lamp depending on the wavelength range desired. Signal output and wavelength were recorded by computer using an Analog Devices Micromac-4000 analog to digital processor. This system allows fast, automatic collection of absorption data.

In order to determine the relationship between chlorine content of the samples and absorption a systematic survey of the available material was made. Absorption data was taken in the visible region for seven samples of

varying dopant concentrations. No data was taken for wavelengths below 500 nM because the samples all showed photoacoustic saturation at this point.

Following the absorption study, photoconductivity measurements were made on the material. The apparatus used is shown in Fig. 2. The sample container was constructed to shield the specimens and provide good electrical contacts while allowing the samples to be changed easily. The optical system described for the PAS system was used here also. A constant voltage was applied to the sample by a Hewlett-Packard regulated power supply and the output current measured by a Keithley current amplifier and recorded by computer. The current amplifier provided gains of up to 10^{11} so very small signals could be detected.

The samples used were all pressed powder pellets and making reliable electrical contacts to these was difficult. The method used was to evaporate gold onto one face of the pellet, masking it with a wire of .040 inches diameter so that a conduction path of constant dimensions was produced (See Fig. 3). Copper contact wires were then attached to the gold with silver contact paint. The small copper contact wires were connected to the leads in the sample holder. This method provided good contact but was difficult due to the extremely fragile nature of the pellets.

As with absorption, photoconductivity data was taken on samples with a range of dopant concentrations. Optimal results were achieved by keeping the samples in total darkness, with 10.0 volts applied, for 24 hrs., then scanning the visible region slowly (3.5 nM per min.).

The photoconductivity spectrum of one pressure quenched sample was investigated. Shortly after pressure quenching the photoconductivity of

this sample was measured in the same manner as the other samples, except the evaporation of gold onto the surface was foregone.

RESULTS

1. Absorption Edge

Optical absorption curves for the various materials are shown in Figs. 4(i) to 4(xii). All curves are corrected for variation in the incident light intensity. Absorption values are in relative units since the absolute magnitude of the absorption depends on sample size, form and surface conditions which were different from one another. The prominent feature of all the curves is the absorption edge which rises steeply as wavelength decreases. The sharpness of the edge varies as did the strength of the output signal. The wavelengths at which the absorptions occur are noticeably shifted for different dopant concentrations. We take the absorption edge to be the point at which the absorption vs. wavelength curve reaches its maximum slope with decreasing wavelength.

We note that the knee occurs at the same chlorine concentration at which the anomalous diamagnetic effects are observed. Figure 5 is a plot of the position of the absorption edge vs. the dopant concentrations. The curve shows a decrease in the photon energy at which the edge occurs with increasing chlorine content. The shift is small at first, then increases at high concentrations.

2. Photoconductivity

Photoconductivity curves are shown in Figs. 6(i) to 6(vi). Each CdS sample has a characteristic peak wavelength where the photocurrent reaches a maximum value. Like the absorption spectra, these were consistently reproducible for the samples tested. Figure 7 is a plot of the position of

the photocurrent maximum vs. dopant concentration. There appear to be two trends from this curve. Initially there is a sharp decrease in the energy at which the maximum occurs, followed by a somewhat more gradual increase which passes through a maximum at high dopant levels. (Unfortunately no data is available for the middle range of concentration due to problems with sample preparation for these materials.)

We note however that again the energy of the maximum photoresponse passes through a maximum at the same chlorine concentration at which the anomalous diamagnetism is observed.

The photoconductivity spectrum for a sample which had been pressure quenched was also investigated and is shown in Fig. 8. Note that this material shows two peaks, the larger of which falls at a much lower photon energy than any of the other samples. It is also interesting to note that the shoulder, which peaks at 625 nM, corresponds to the peak of a sample of similar composition which was not pressure quenched. This peak disappeared with time while the large peak became sharper and moved to longer wavelengths, as seen in Fig. 9 which shows data taken 3 months later.

DISCUSSION

1. Absorption

In a pure, perfect crystal of CdS the optical absorption spectrum should have only one feature; a sharply defined edge at 520 nM wavelength. This would correspond to optically excited transitions across the fundamental energy gap of 2.4 eV. In real crystals there are a number of defects such as Cd and S vacancies which result in defect states within the forbidden gap. The effect of these states is a loss of sharpness in the absorption edge

caused by the existence of smaller absorption peaks near the edge which correspond to transitions to and from states within the energy gap. The incorporation of the halide impurity, Cl, creates another level of states in the gap which lies very near (about .05 eV) the edge of the conduction band. The Cl impurities act as donors, each giving up an electron to the conduction band. This excess of electrons, which is quite large in heavily doped material, increases the conductivity and also serves to fill many of the defect states in the gap. The filled states become negatively charged giving them a large hole capture cross section and small electron capture cross section which results in increased decay time and greater photoconductivity.[3]

In our work it was observed that the Cl impurities also result in a shift of the apparent absorption edge to longer wavelengths with increasing concentration. The shift is small for dopant concentrations of up to .72% and is readily explained by the model described above as follows.

At room temperature many of the chlorine donor states will be ionized. These empty states will accept electrons photoexcited from the valence band. The energy required to promote such an electron from the valence band edge to the empty Cl impurity level is .05 eV smaller than that needed for a band to band transition. Ideally an absorption peak, probably of gaussian shape since the Cl level is not perfectly sharp, will result just below the fundamental absorption edge due to these transitions from the valence band into the empty chlorine donor states. The growth in height of this gaussian absorption peak gives rise to an apparent shifting with increasing chlorine concentration of the edge towards longer wavelengths. Figure 5 shows that the extent of this broadening reaches .05 eV at .72% Cl, suggesting that at

this point the absorption from the Cl states is very strong.

At a concentration of .72%, there is an abrupt change in the concentration dependence of the apparent edge shift. We postulate that an impurity band is formed at .72 wt.%, which will of course widen with increasing chlorine content as the mean overlap between centers increases with decreasing distance.

It is interesting to note that the change in curvature occurs at the same Cl concentration at which the large diamagnetism was observed, which again suggests the occurrence of an unusual electronic state.

2. Photoconductivity

The spectral response of the photocurrent of a semiconductor should closely resemble the absorption spectrum, in the ideal case where the only transition occurring is band to band. In practice there are numerous defect states in the energy gap as mentioned earlier. The relative population of states not only allow other electronic transitions but also modify the recombination processes.

For lack of sufficient evidence at the present time, we might conjecture that the increase in energy at the maximum photo-response comes about by the larger number of holes, formed by photo-excitation into the empty chlorine levels, increasing the density of active recombination centers. This would result in a decreased lifetime of the majority negative carriers. Beyond .80% Cl, where the impurity band is believed to have formed and overlap the conduction band, increasing the dopant concentration broadens the band which has the effect of narrowing the gap and consequently moving the photo-current peak to lower energies, as shown by the last two points.

In Fig. 8 the photoconductivity spectra of doped pressure quenched material is shown. Two peaks are evident for the quenched material, the

smaller one appearing as a shoulder at 620 nM. This is consistent with the known structure of the pressure quenched material, namely that after pressure quenching two phases are present in the CdS, the normal wurtzite structure and the high pressure NaCl structure. The latter, being a cubic structure, will have a narrower energy gap than the original material. This accounts for the large peak at the long wavelength end of the spectrum. The smaller peak occurs at the same wavelength as that for the original material and probably results from the small amount of CdS that has returned to the wurtzite structure. It is interesting to note that a similar experiment run at a later date produced a spectrum in which the smaller peak was absent, indicating that the material is metastable as believed.

REFERENCES

1. E. Brown, C. G. Homan and R. K. MacCrone, Phys. Rev. Lett. 45, 478 (1980).
2. J. A. Corll, J. Appl. Phys. 35, 3032 (1964).
3. R. H. Bube and S. M. Thomsen, J. Chem. Phys. 23, 15 (1955).
4. E. Brown, C. G. Homan and R. K. MacCrone, Phys. Rev. Lett. 45, 478 (1980).
5. S. Bloch and G. Piermarini - private communication.
6. A. Rosencwaig, Photoacoustics and Photoacoustic Spectroscopy, Wiley & Sons, (1980).

TABLE I

CHLORINE CONCENTRATION OF MATERIALS STUDIED

Material	Wt.% Cl	Source
E.P.	0.0	Eagle Pitcher
AI#066278	0.0	Alpha Inorganic
NBS-23	0.10	Natl. Bureau of Standards
NBS-25	0.20	Natl. Bureau of Standards
NBS-31B	0.50	Natl. Bureau of Standards
NBS-8	0.72	Natl. Bureau of Standards
NBS-17	0.93	Natl. Bureau of Standards
NBS-31C	1.20	Natl. Bureau of Standards
NBS-12	2.80	Natl. Bureau of Standards

Figure 1

Schematic of Photoacoustic Spectroscopy System

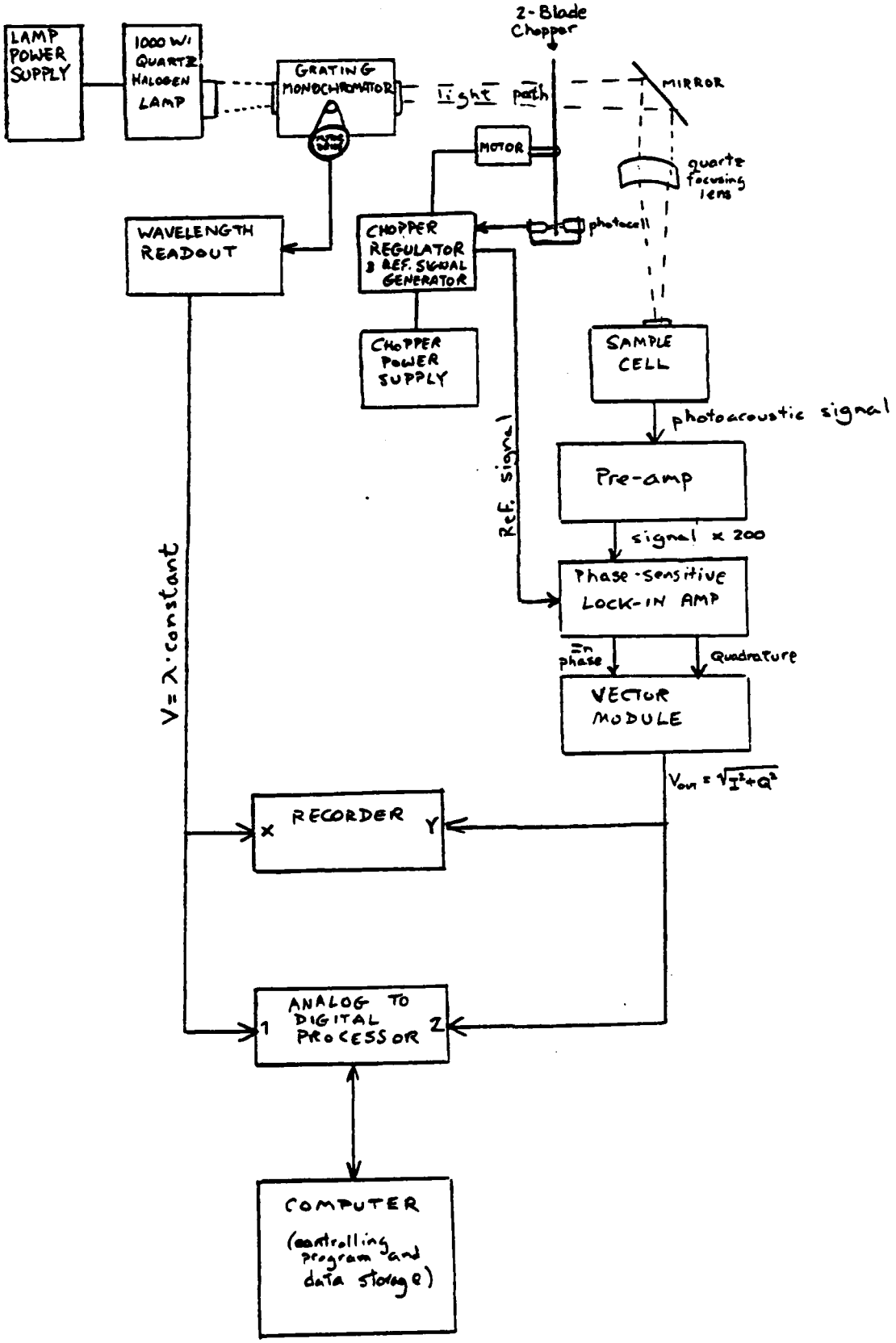

Figure 2

Schematic of Photoconductivity Measurement System

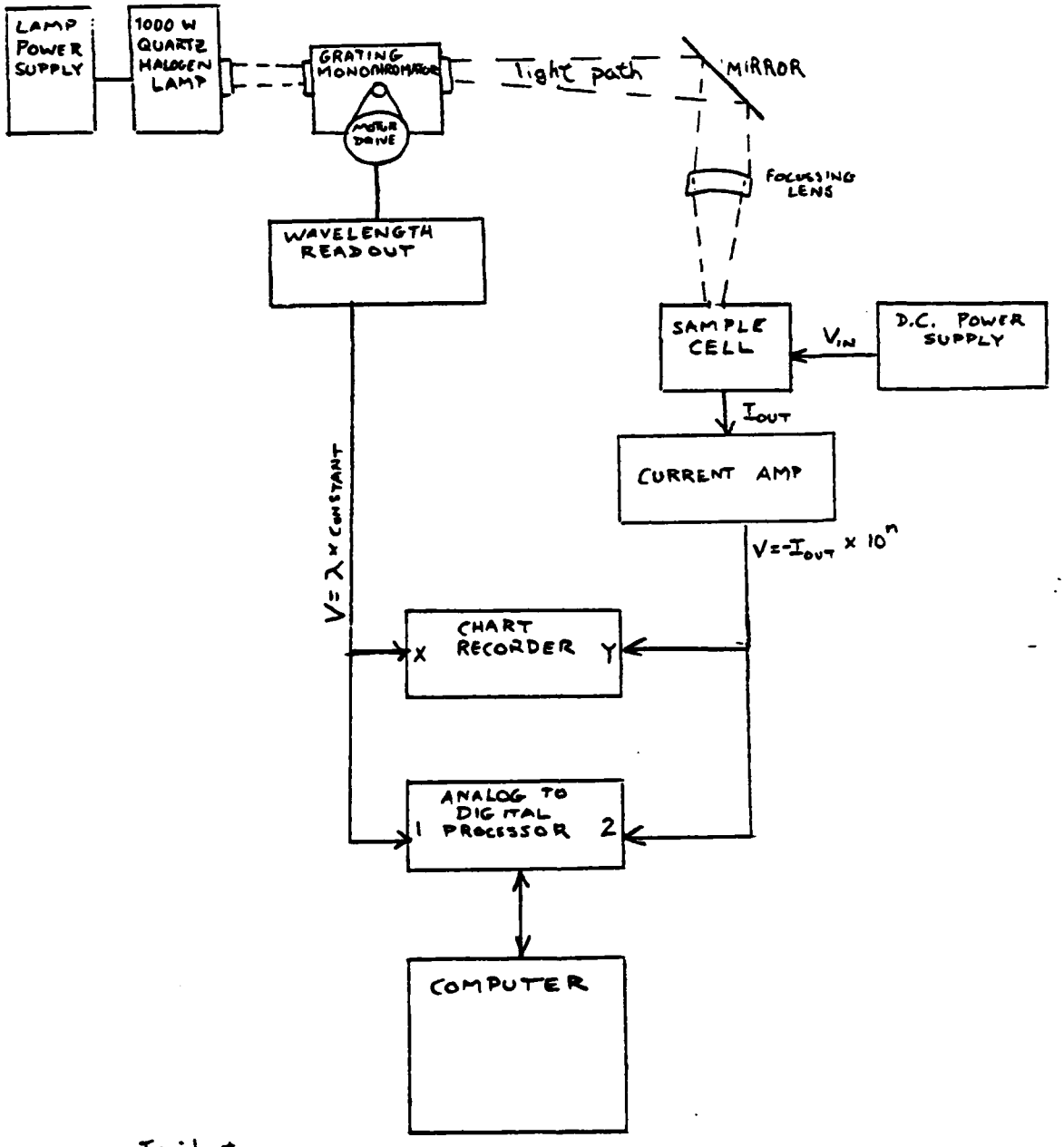

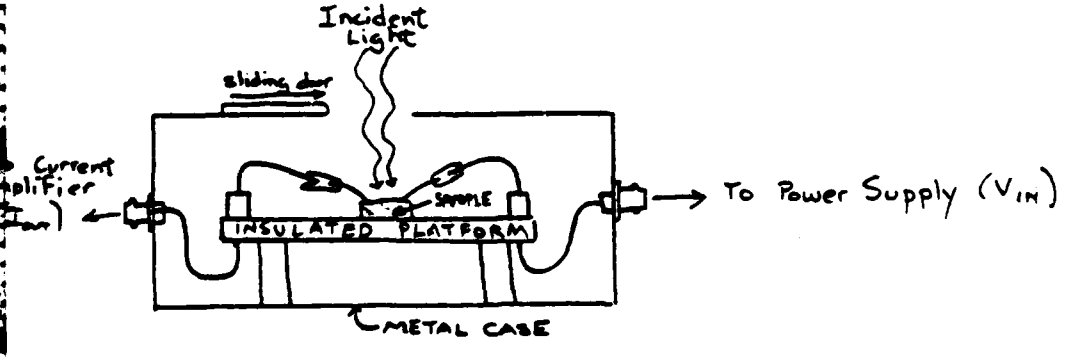

Detail of Sample Cell

Figure 3

Photoconductivity Sample Preparation

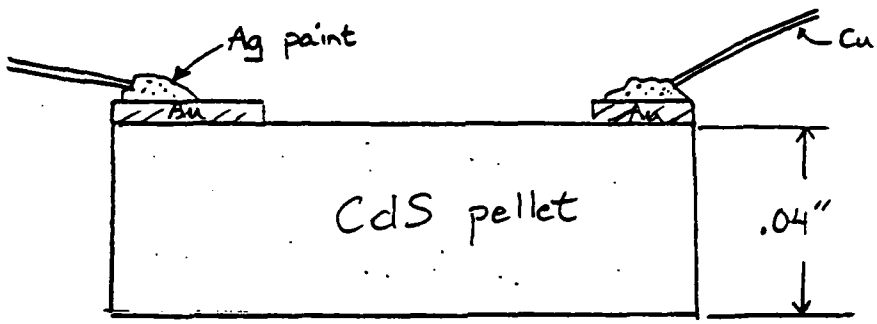

side view of CdS pellet with finished contacts attached (thickness of Au is exagerrated)

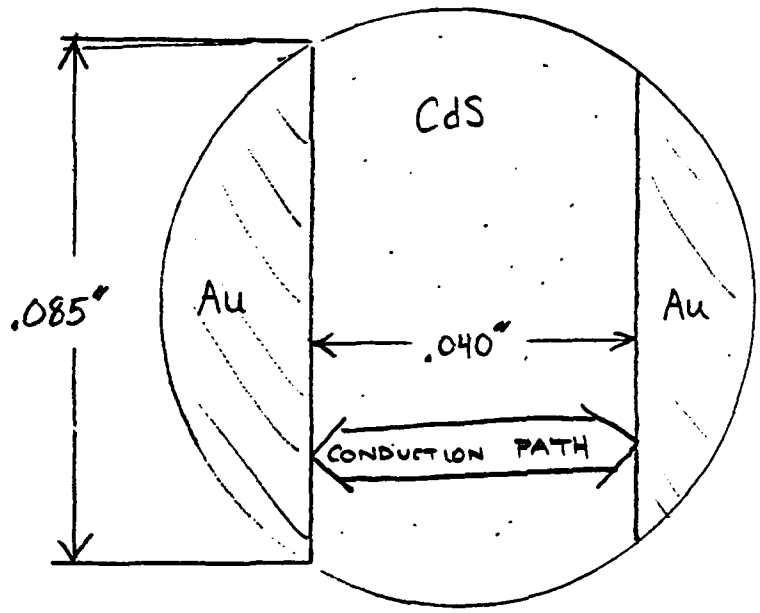

Diameter of pellets ≅ 2.5 mm

Total area of conduction path is ≈ .02 cm^2

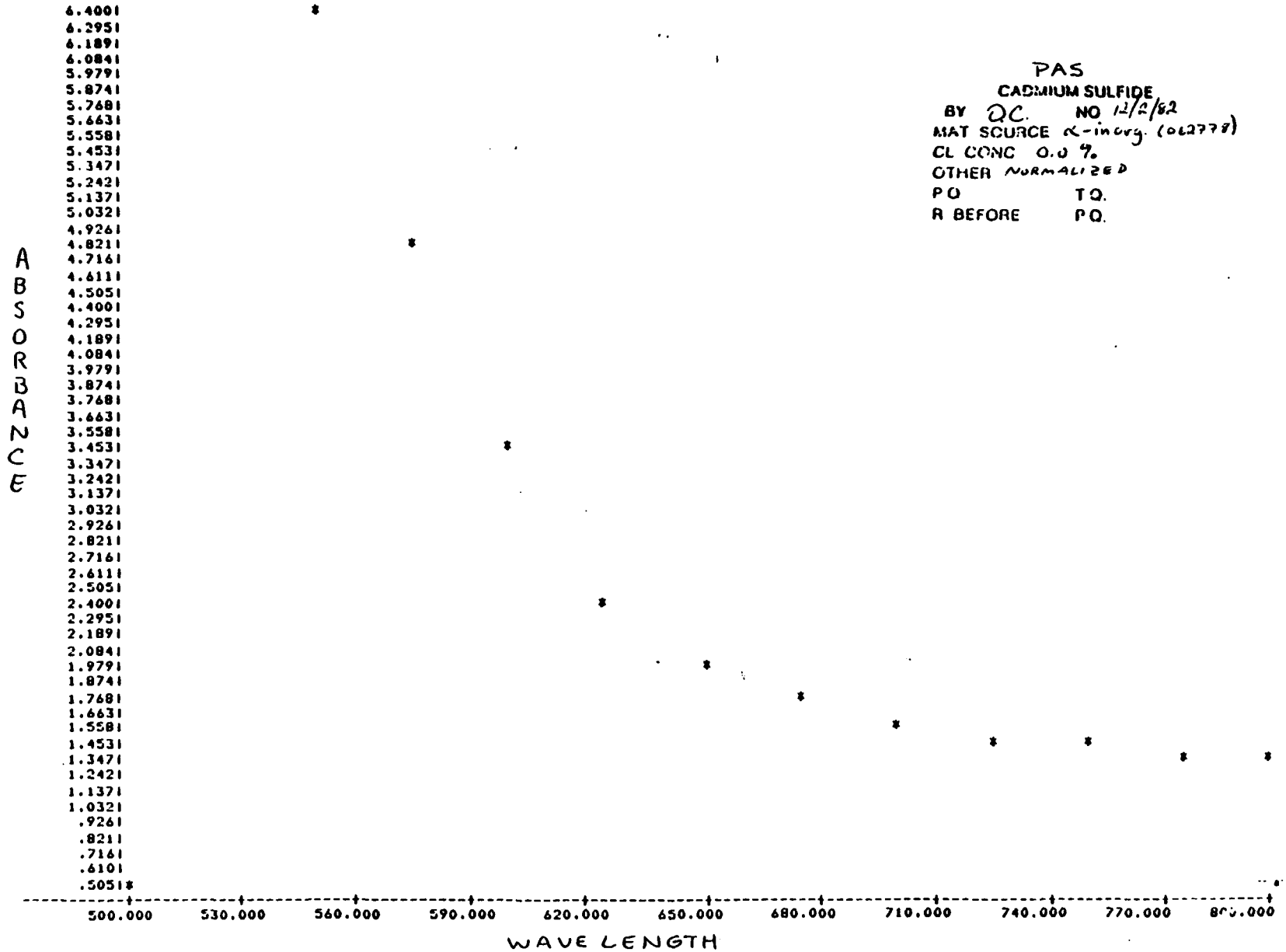

Figure 4(i)

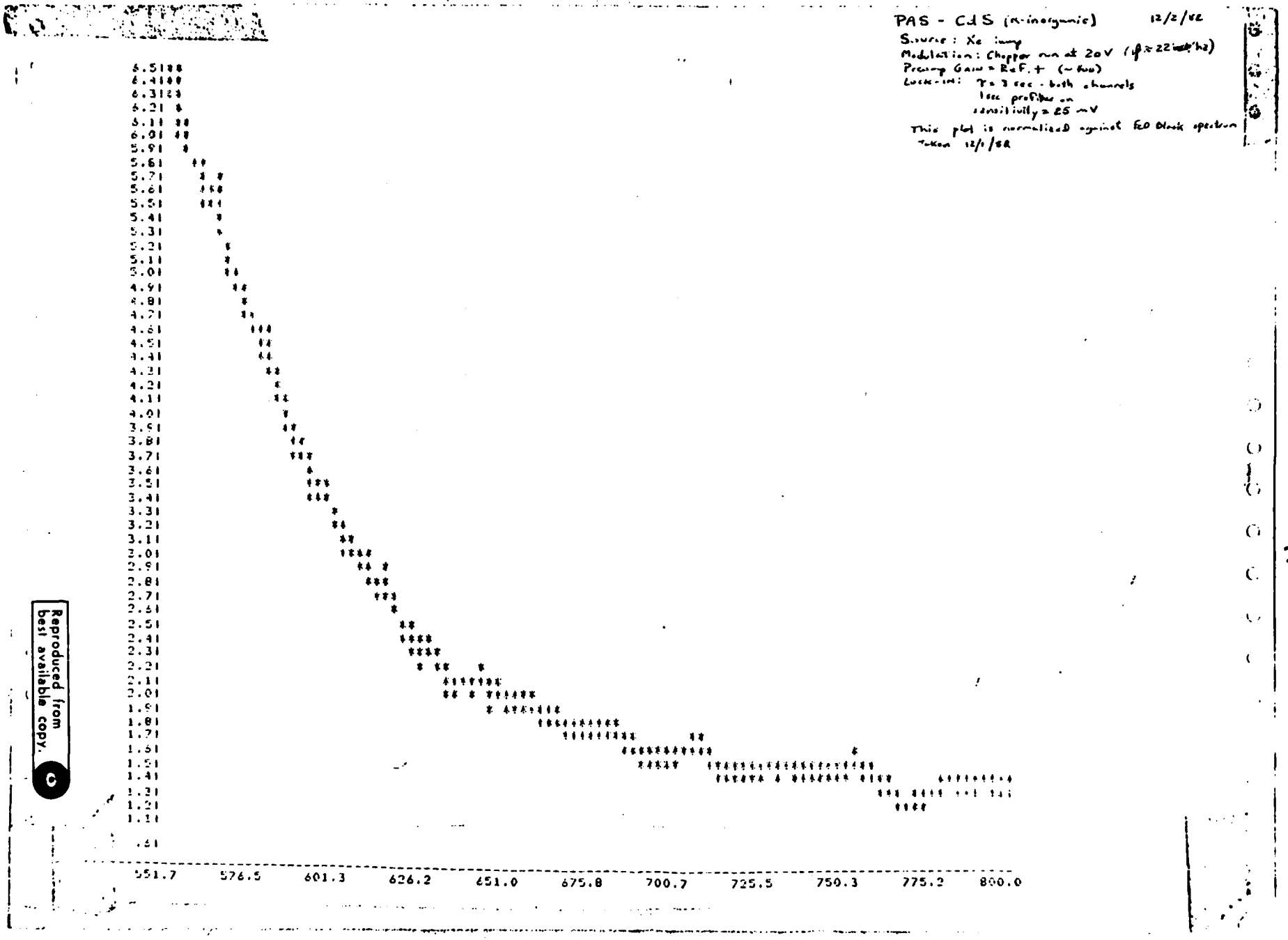

Figure 4(ii)

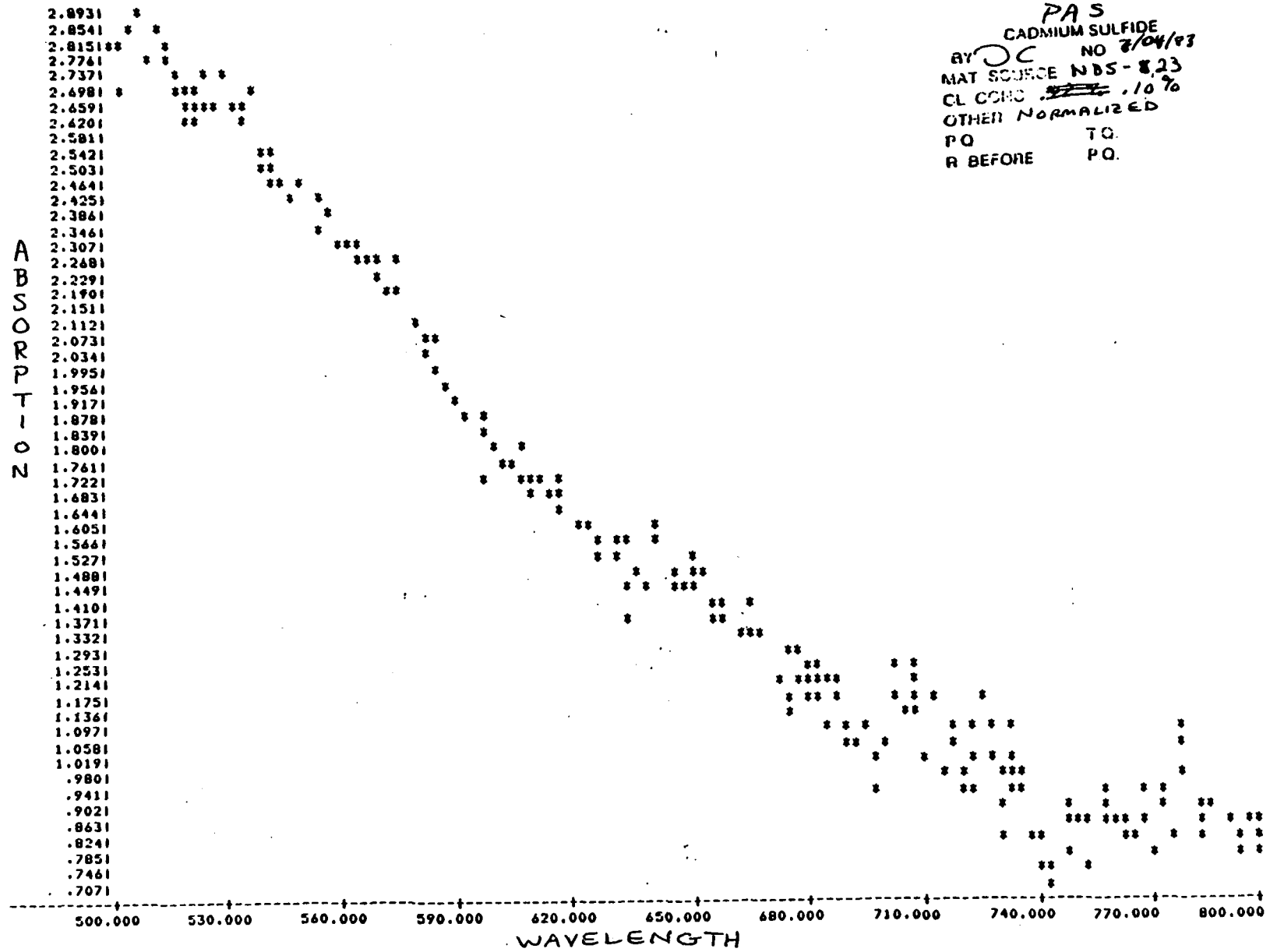
PAS
CADMIUM SULFIDE
BY JC NO 8/04/93
MAT SOURCE NBS - 8,23
CL CONC .10%
OTHER NORMALIZED
P.Q. T.Q.
R BEFORE P.Q.
ABSORPTION
2.8931
2.8541
2.8151
2.7761
2.7371
2.6981
2.6591
2.6201
2.5811
2.5421
2.5031
2.4641
2.4251
2.3861
2.3471
2.3071
2.2681
2.2291
2.1901
2.1511
2.1121
2.0731
2.0341
1.9951
1.9561
1.9171
1.8781
1.8391
1.8001
1.7611
1.7221
1.6831
1.6441
1.6051
1.5661
1.5271
1.4881
1.4491
1.4101
1.3711
1.3321
1.2931
1.2531
1.2141
1.1751
1.1361
1.0971
1.0581
1.0191
.9801
.9411
.9021
.8631
.8241
.7851
.7461
.7071
500.000
530.000
560.000
590.000
620.000
650.000
680.000
710.000
740.000
770.000
800.000
WAVELENGTH

Figure 4(iii)

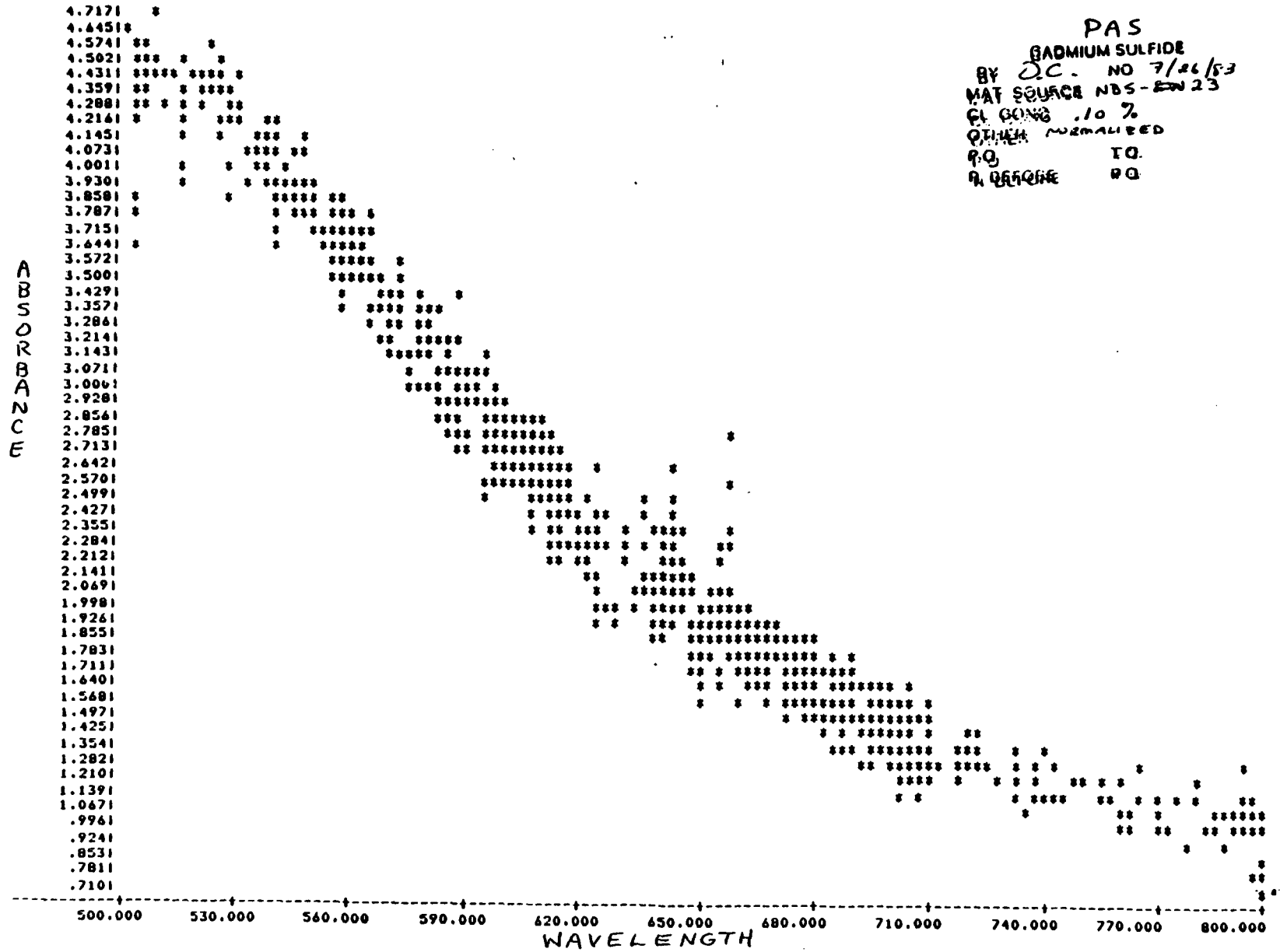
PAS
CADMIUM SULFIDE
BY DC. NO 7/26/83
MAT SOURCE NBS-SRM 23
CL CONC .10 %
QTUBE NORMALIZED
RQ TQ
RA RESCUE RQ
ABSORBANCE
4.7171
4.4451
4.5741
4.5021
4.4311
4.3591
4.2881
4.2161
4.1451
4.0731
4.0011
3.9301
3.8581
3.7871
3.7151
3.6441
3.5721
3.5001
3.4291
3.3571
3.2861
3.2141
3.1431
3.0711
3.0001
2.9281
2.8561
2.7851
2.7131
2.6421
2.5701
2.4991
2.4271
2.3551
2.2841
2.2121
2.1411
2.0691
1.9981
1.9261
1.8551
1.7831
1.7111
1.6401
1.5681
1.4971
1.4251
1.3541
1.2821
1.2101
1.1391
1.0671
.9961
.9241
.8531
.7811
.7101
500.000
530.000
560.000
590.000
620.000
650.000
680.000
710.000
740.000
770.000
800.000
WAVELENGTH

Figure 4(iv)

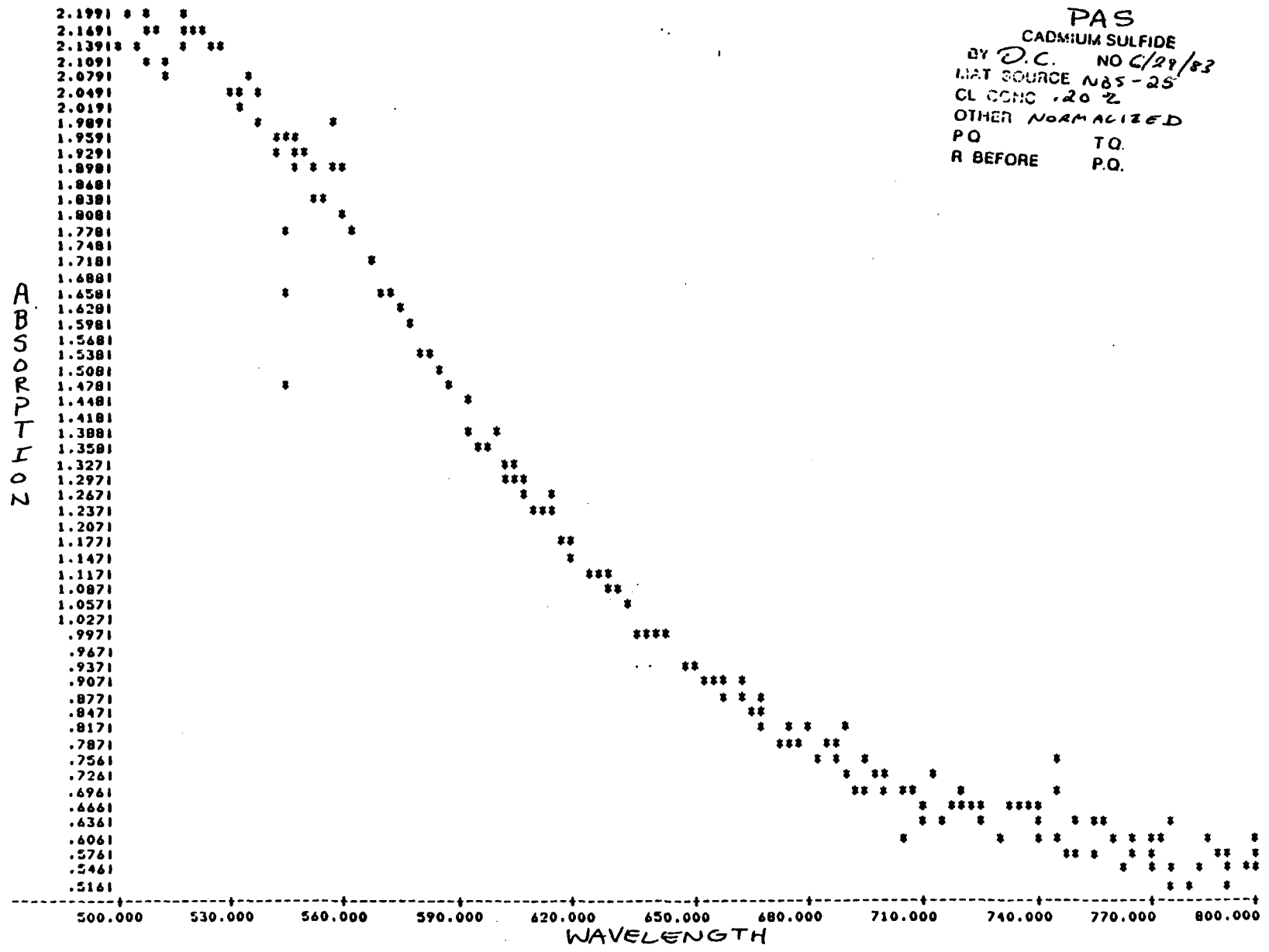
PAS
CADMIUM SULFIDE
BY D.C. NO C/29/83
MAT SOURCE N85-25
CL CONC .20 %
OTHER NORMALIZED
P.Q. T.Q.
R BEFORE P.Q.
ABSORPTION
2.199
2.169
2.139
2.109
2.079
2.049
2.019
1.989
1.959
1.929
1.898
1.868
1.838
1.808
1.778
1.748
1.718
1.688
1.658
1.628
1.598
1.568
1.538
1.508
1.478
1.448
1.418
1.388
1.358
1.327
1.297
1.267
1.237
1.207
1.177
1.147
1.117
1.087
1.057
1.027
.997
.967
.937
.907
.877
.847
.817
.787
.756
.726
.696
.666
.636
.606
.576
.546
.516
500.000
530.000
560.000
590.000
620.000
650.000
680.000
710.000
740.000
770.000
800.000
WAVELENGTH

Figure 4(v)

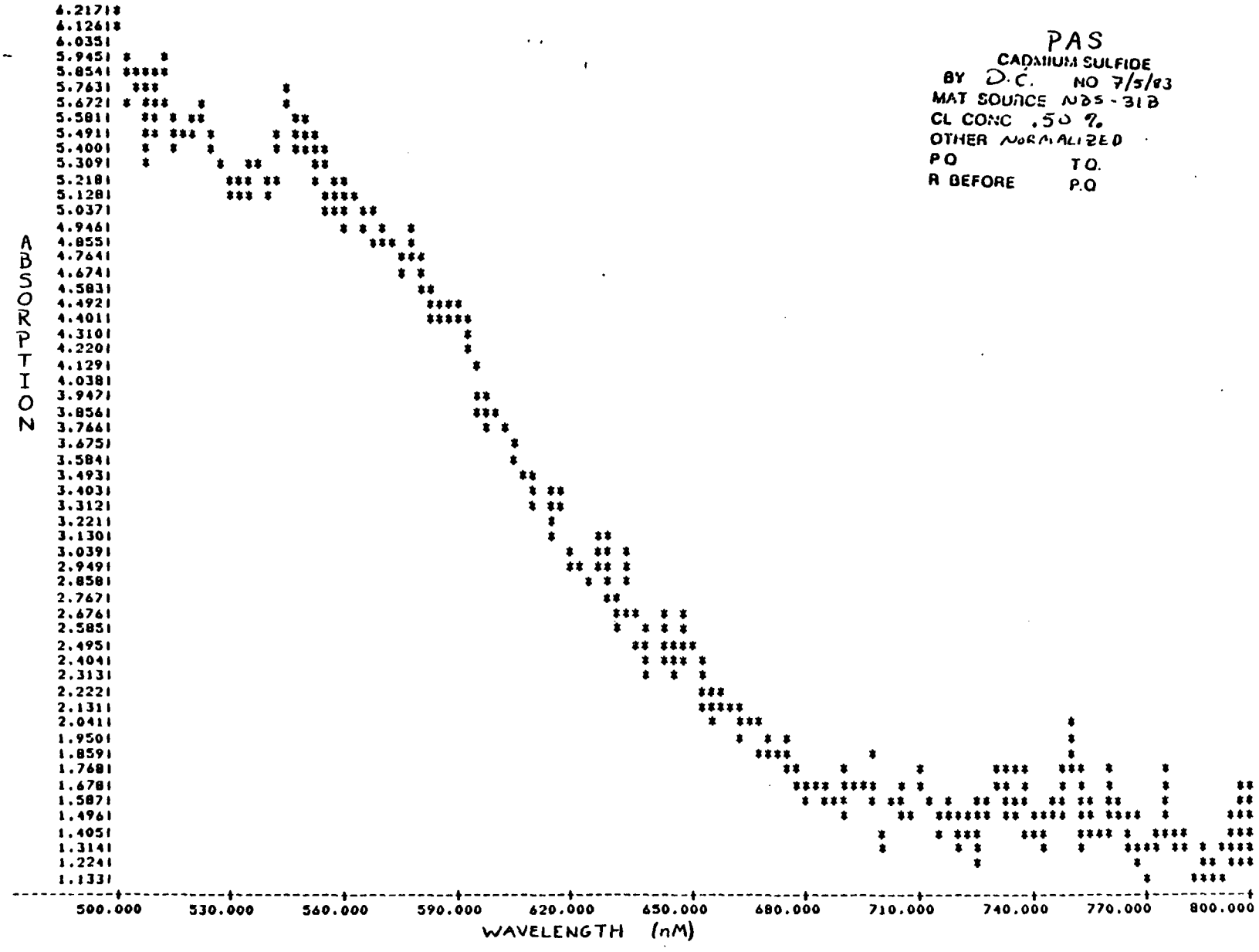
PAS
CADMIUM SULFIDE
BY D.C. NO 7/5/83
MAT SOURCE NBS-31B
CL CONC .50 %
OTHER NORMALIZED
P O T O.
R BEFORE P.O
ABSORPTION
4.2171
4.1261
4.0351
5.9451
5.8541
5.7631
5.6721
5.5811
5.4911
5.4001
5.3091
5.2181
5.1281
5.0371
4.9461
4.8551
4.7641
4.6741
4.5831
4.4921
4.4011
4.3101
4.2201
4.1291
4.0381
3.9471
3.8561
3.7661
3.6751
3.5841
3.4931
3.4031
3.3121
3.2211
3.1301
3.0391
2.9491
2.8581
2.7671
2.6761
2.5851
2.4951
2.4041
2.3131
2.2221
2.1311
2.0411
1.9501
1.8591
1.7681
1.6781
1.5871
1.4961
1.4051
1.3141
1.2241
1.1331
500.000
530.000
560.000
590.000
620.000
650.000
680.000
710.000
740.000
770.000
800.000
WAVELENGTH (nM)

Figure 4(vi)

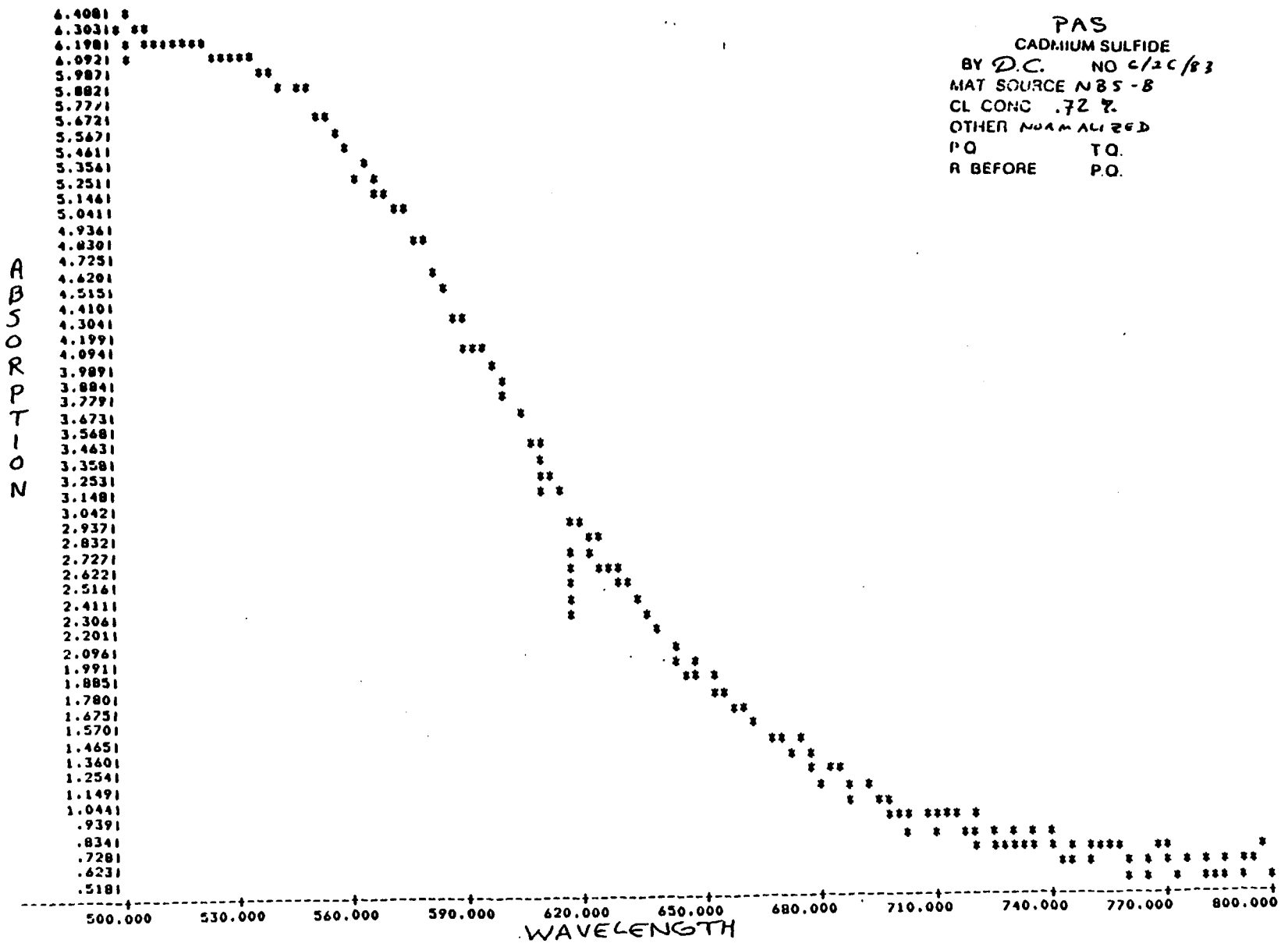
PAS
CADMIUM SULFIDE
BY D.C. NO 6/26/83
MAT SOURCE NBS-B
CL CONC .72 %
OTHER NORMALIZED
P.O. T.O.
R BEFORE P.O.
ABSORPTION
WAVELENGTH
500.000
530.000
560.000
590.000
620.000
650.000
680.000
710.000
740.000
770.000
800.000

Figure 4(vii)

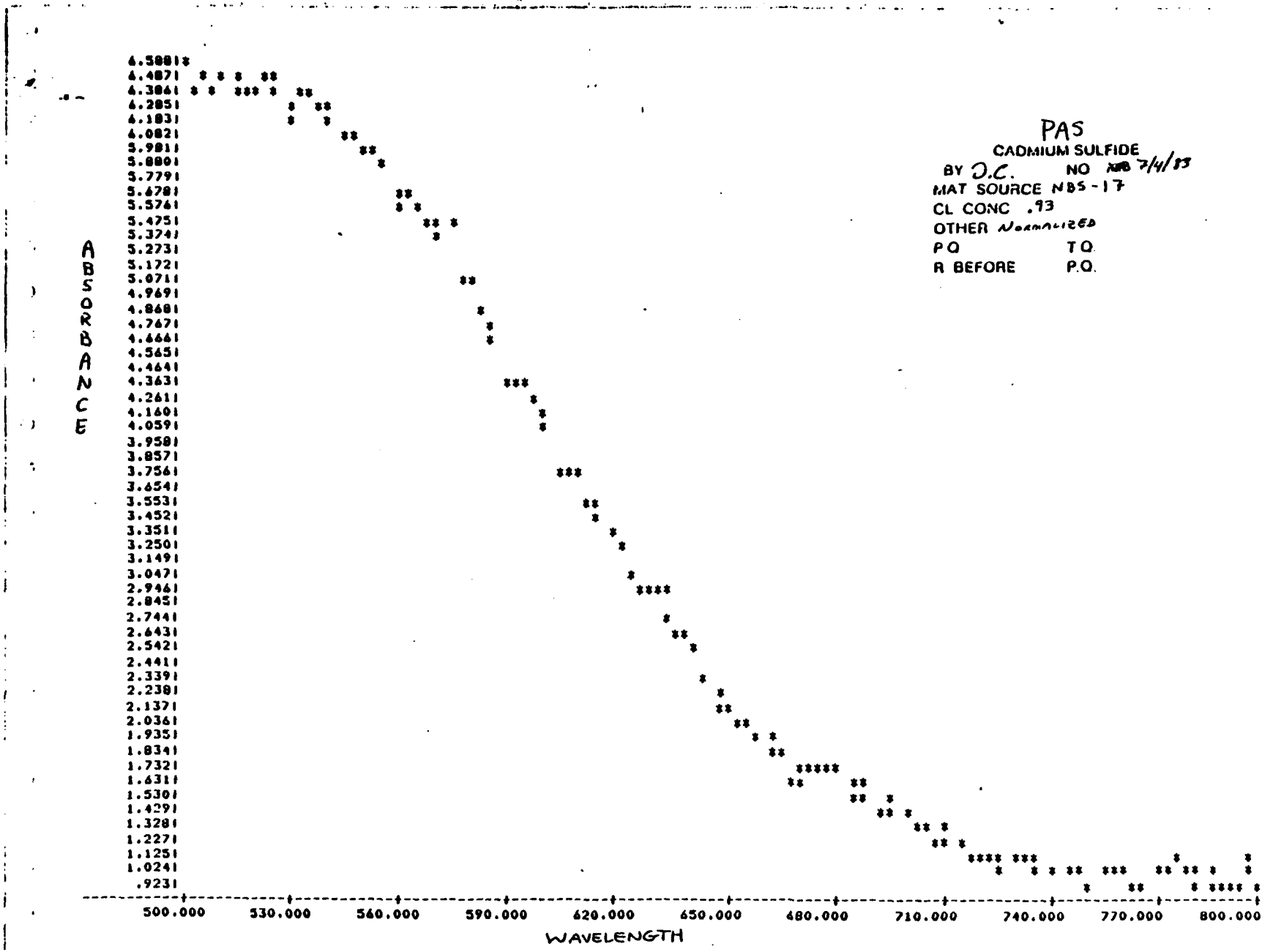

Figure 4(viii)

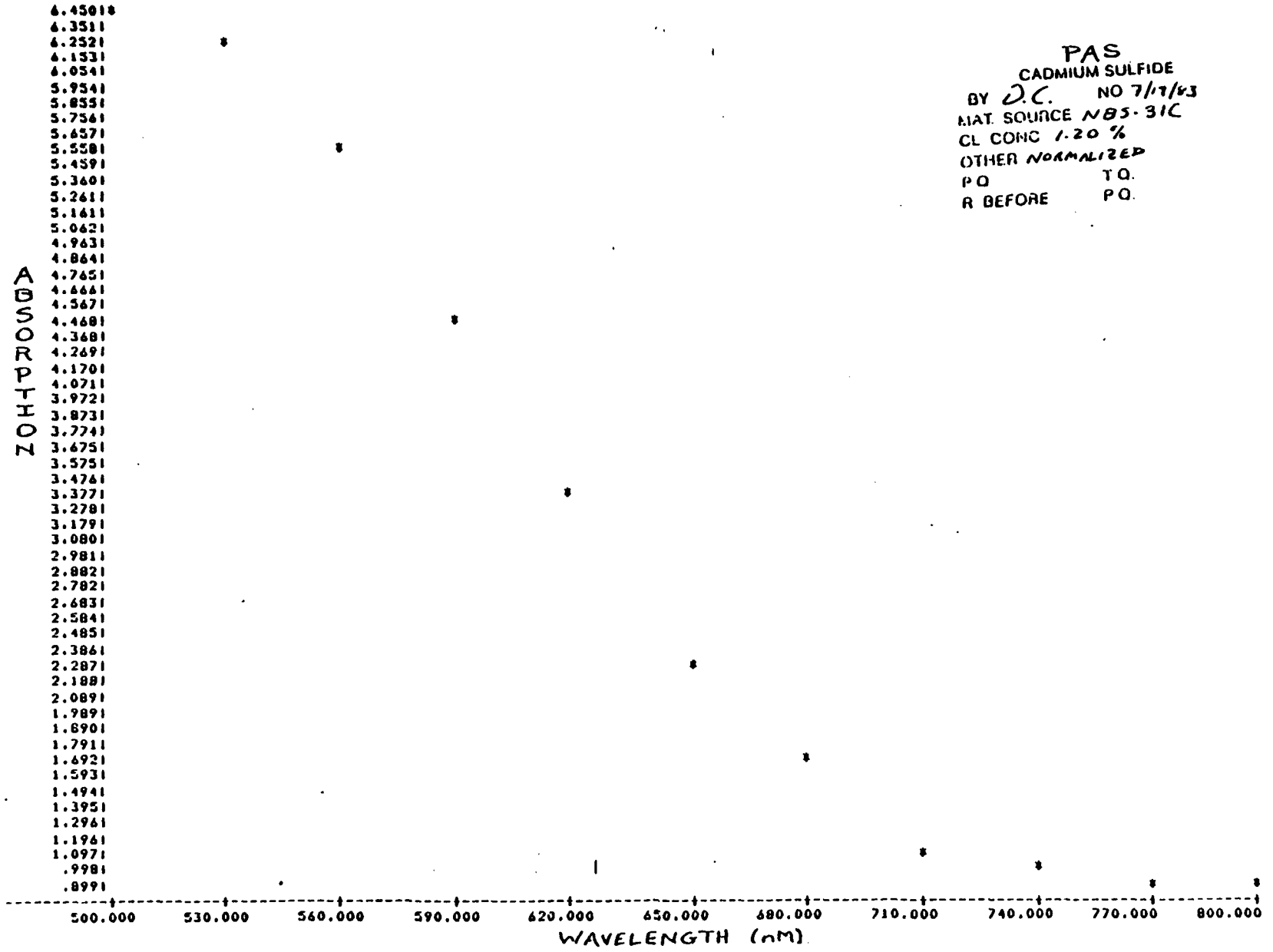
PAS
CADMIUM SULFIDE
BY D.C. NO 7/17/83
MAT. SOURCE NBS-31C
CL CONC 1.20 %
OTHER NORMALIZED
P Q T Q.
R BEFORE P Q.
ABSORPTION
6.4501
6.3511
6.2521
6.1531
6.0541
5.9541
5.8551
5.7561
5.6571
5.5581
5.4591
5.3601
5.2611
5.1611
5.0621
4.9631
4.8641
4.7651
4.6661
4.5671
4.4681
4.3681
4.2691
4.1701
4.0711
3.9721
3.8731
3.7741
3.6751
3.5751
3.4761
3.3771
3.2781
3.1791
3.0801
2.9811
2.8821
2.7821
2.6831
2.5841
2.4851
2.3861
2.2871
2.1881
2.0891
1.9891
1.8901
1.7911
1.6921
1.5931
1.4941
1.3951
1.2961
1.1961
1.0971
.9981
.8991
500.000
530.000
560.000
590.000
620.000
650.000
680.000
710.000
740.000
770.000
800.000
WAVELENGTH (nM)

Figure 4(ix)

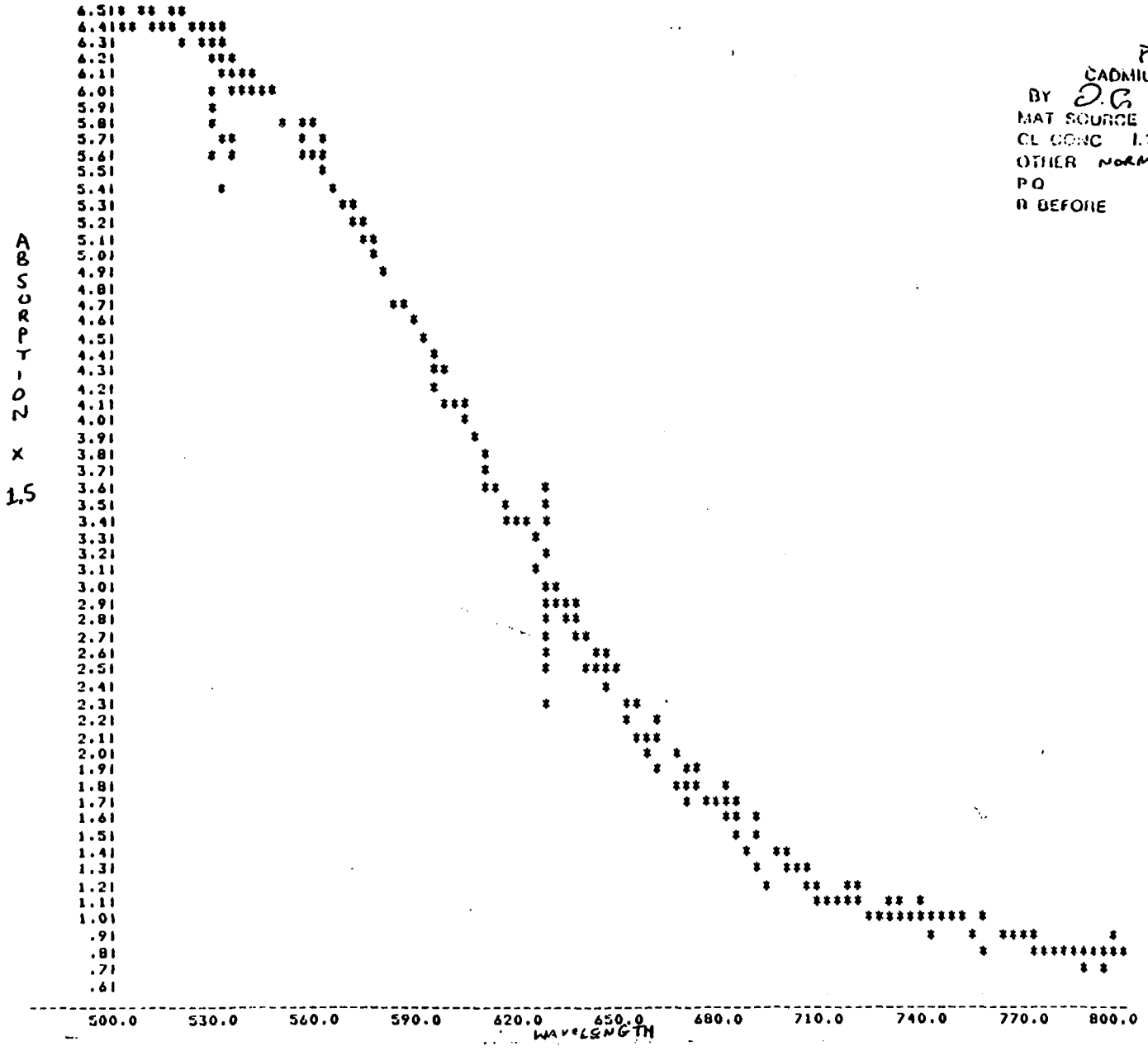
PAS
CADMIUM SULFIDE
BY D.G NO 7/1/83
MAT SOURCE NBS-31C
CL CONC 1.20 %
OTHER NORM.
PO TO
B BEFORE PO
ABSORPTION X 1.5
WAVELENGTH
500.0
530.0
560.0
590.0
620.0
650.0
680.0
710.0
740.0
770.0
800.0

Figure 4(x)

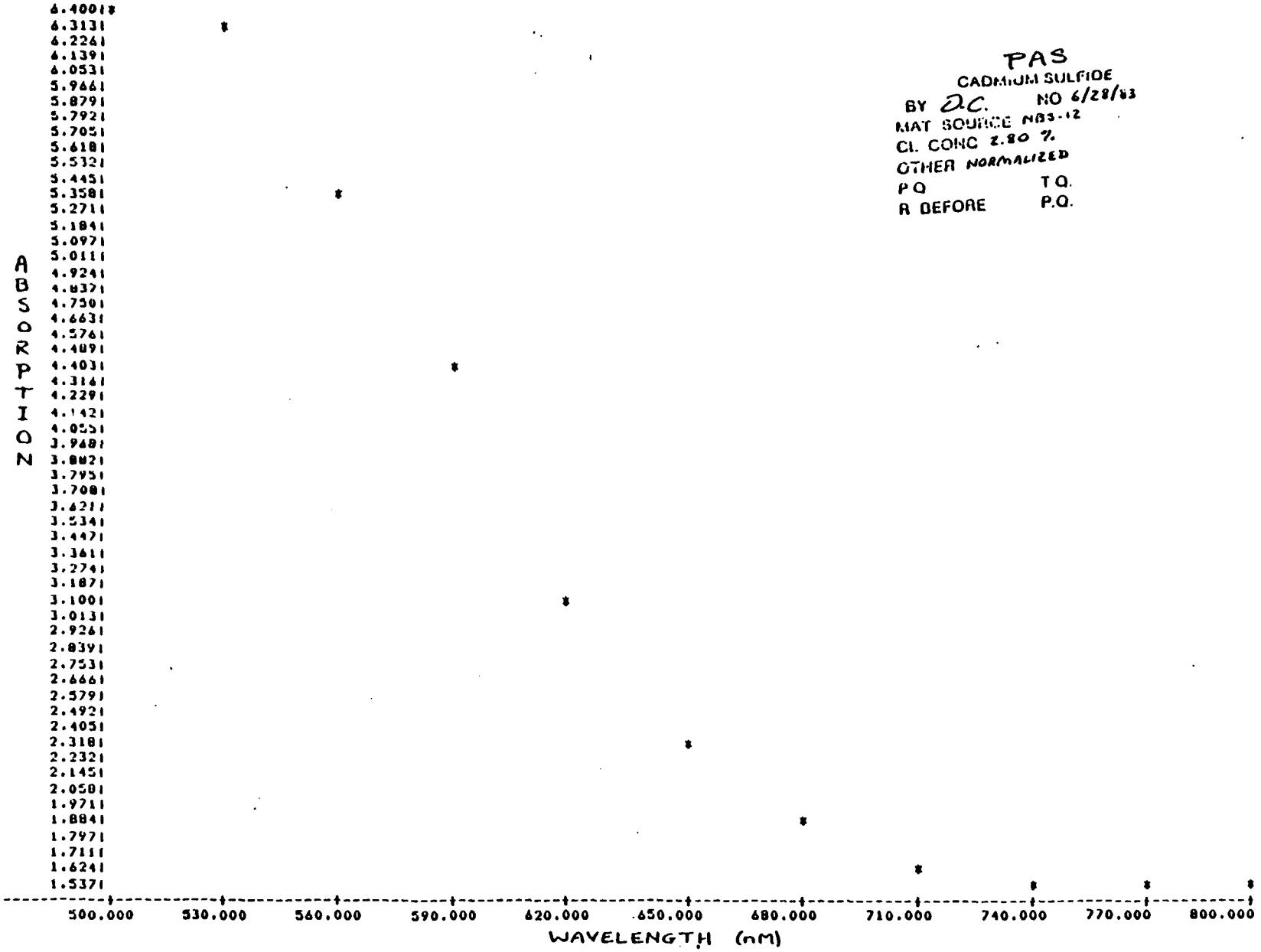
PAS
CADMIUM SULFIDE
BY ac. NO 6/28/83
MAT SOURCE NBS-12
CL. CONC 2.80 %
OTHER NORMALIZED
P.Q T.Q.
R BEFORE P.Q.
ABSORPTION
6.400
6.313
6.226
6.139
6.053
5.966
5.879
5.792
5.705
5.618
5.532
5.445
5.358
5.271
5.184
5.097
5.011
4.924
4.837
4.750
4.663
4.576
4.489
4.403
4.316
4.229
4.142
4.055
3.968
3.882
3.795
3.708
3.621
3.534
3.447
3.361
3.274
3.187
3.100
3.013
2.926
2.839
2.753
2.666
2.579
2.492
2.405
2.318
2.232
2.145
2.058
1.971
1.884
1.797
1.711
1.624
1.537
500.000
530.000
560.000
590.000
620.000
650.000
680.000
710.000
740.000
770.000
800.000
WAVELENGTH (nM)

Figure 4(xi)

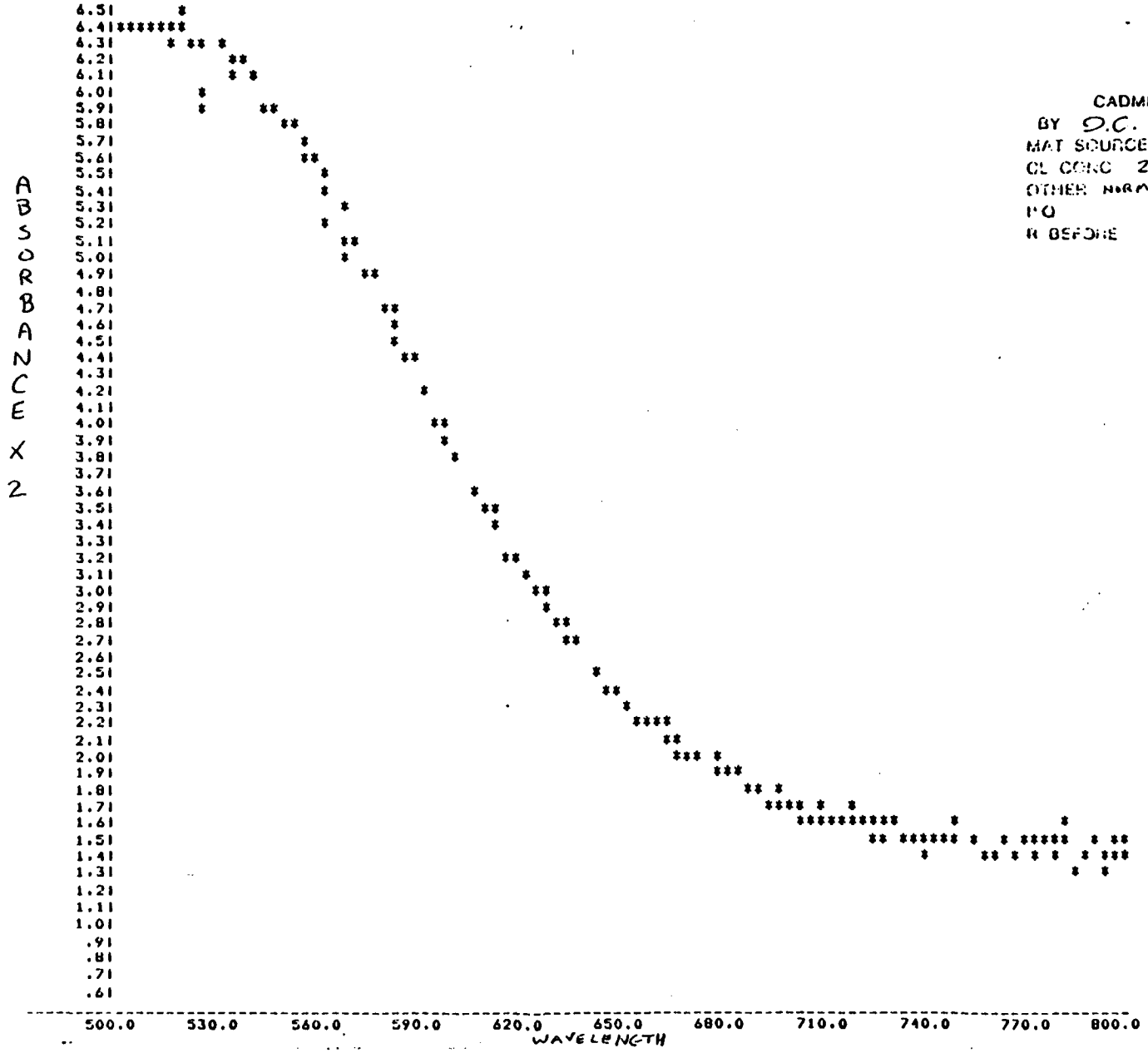
PAS
CADMIUM SULFIDE
BY D.C. NO
MAT SOURCE NBC-12
CL CONC 2.80 %
OTHER NORMALIZED
PO TO
R BEFORE PO
ABSORBANCE X 2
6.51
6.41
6.31
6.21
6.11
6.01
5.91
5.81
5.71
5.61
5.51
5.41
5.31
5.21
5.11
5.01
4.91
4.81
4.71
4.61
4.51
4.41
4.31
4.21
4.11
4.01
3.91
3.81
3.71
3.61
3.51
3.41
3.31
3.21
3.11
3.01
2.91
2.81
2.71
2.61
2.51
2.41
2.31
2.21
2.11
2.01
1.91
1.81
1.71
1.61
1.51
1.41
1.31
1.21
1.11
1.01
.91
.81
.71
.61
500.0
530.0
560.0
590.0
620.0
650.0
680.0
710.0
740.0
770.0
800.0
WAVELENGTH

Figure 4(xii)

CADMIUM SULFIDE

ABSORPTION EDGE vs Cl CONTENT

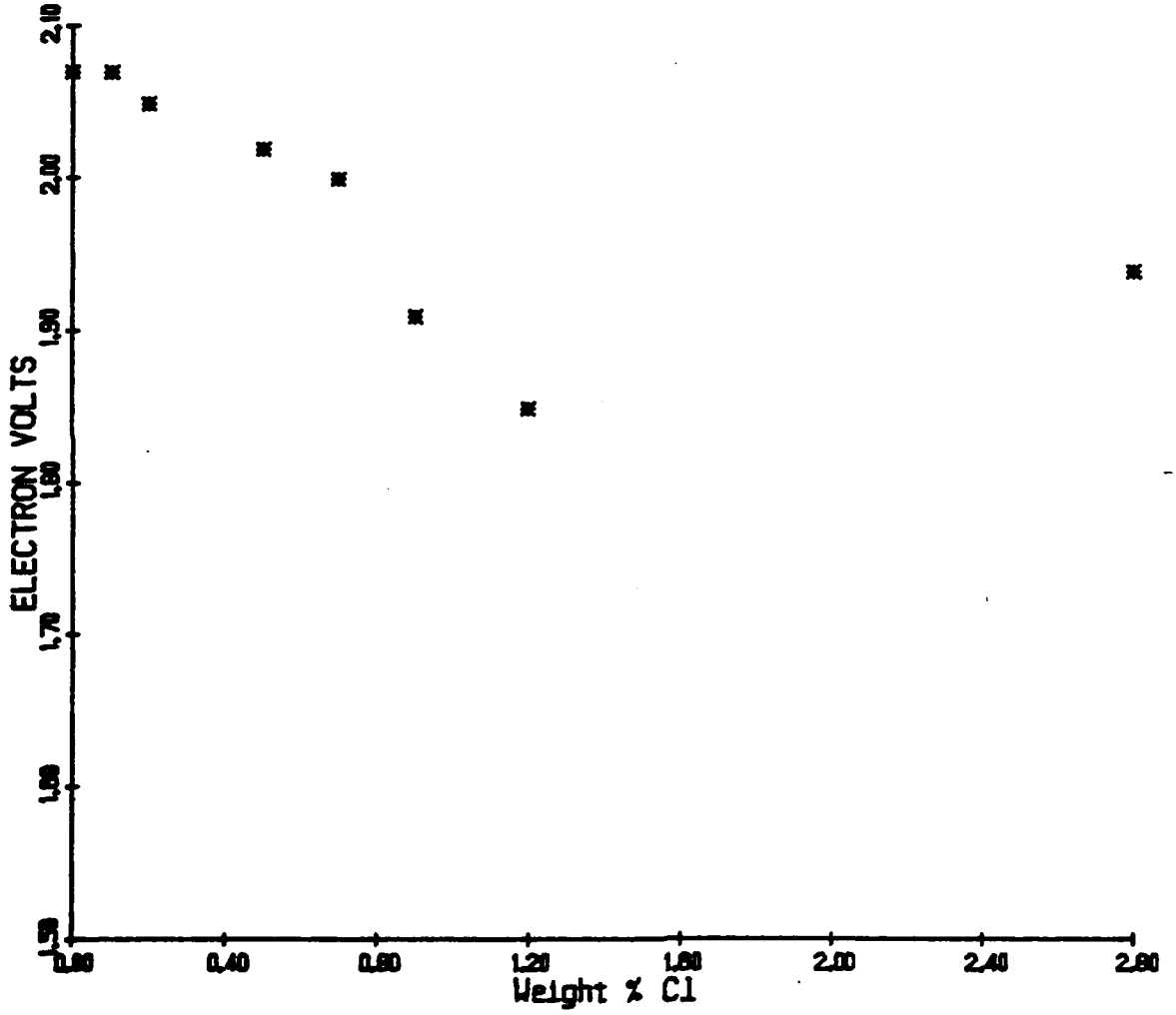

Photoconductivity of CdS (E.P.)

5/4/13

* Corrected for variations in light source intensity

CADMIUM SULFIDE
BY D. Campbell NO
MAT SOURCE Eagle-Pitcher
CL CONC 0.0 %
OTHER NORMALIZED
P Q T Q
R BEFORE P O

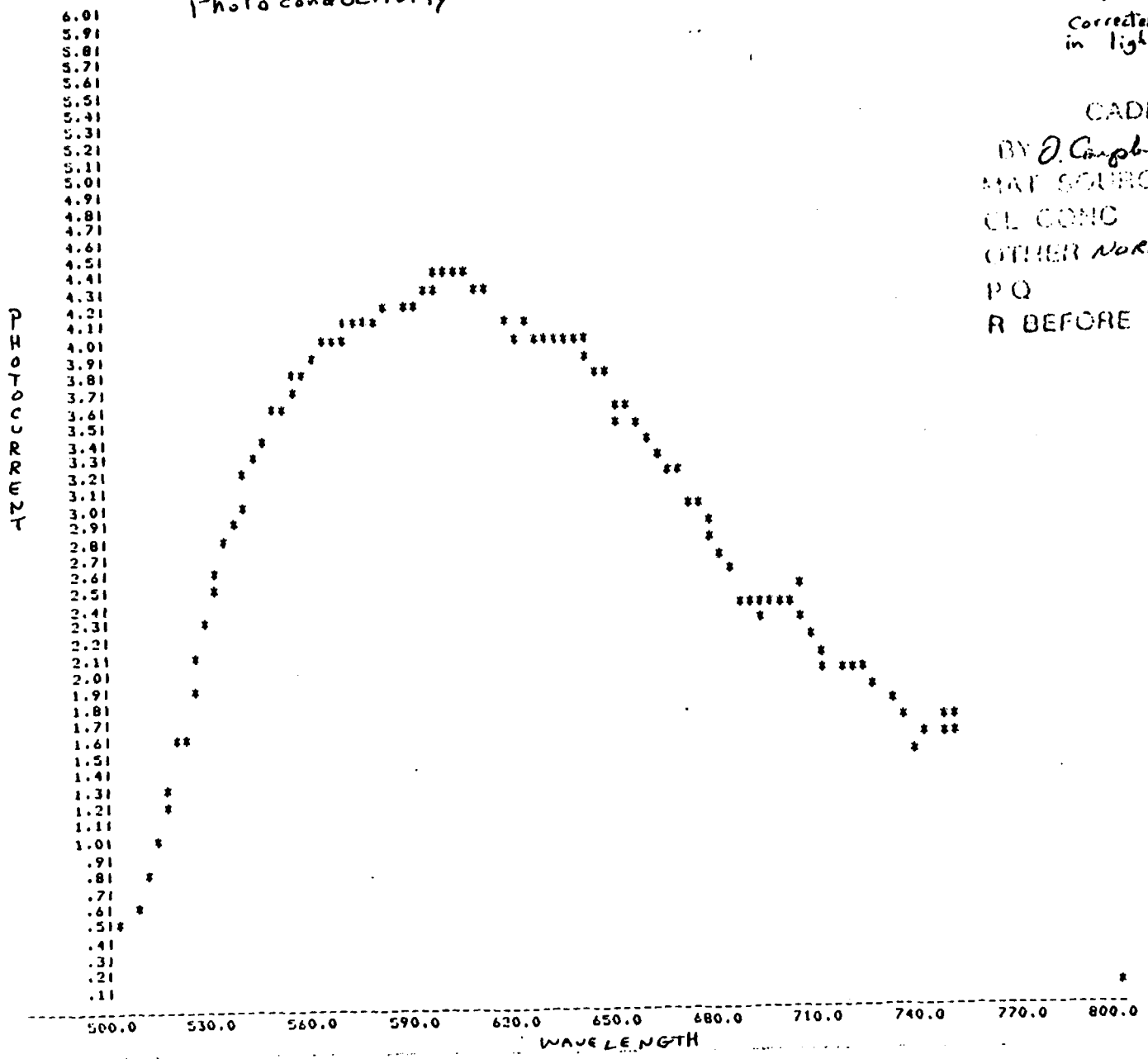

Figure 6(i)

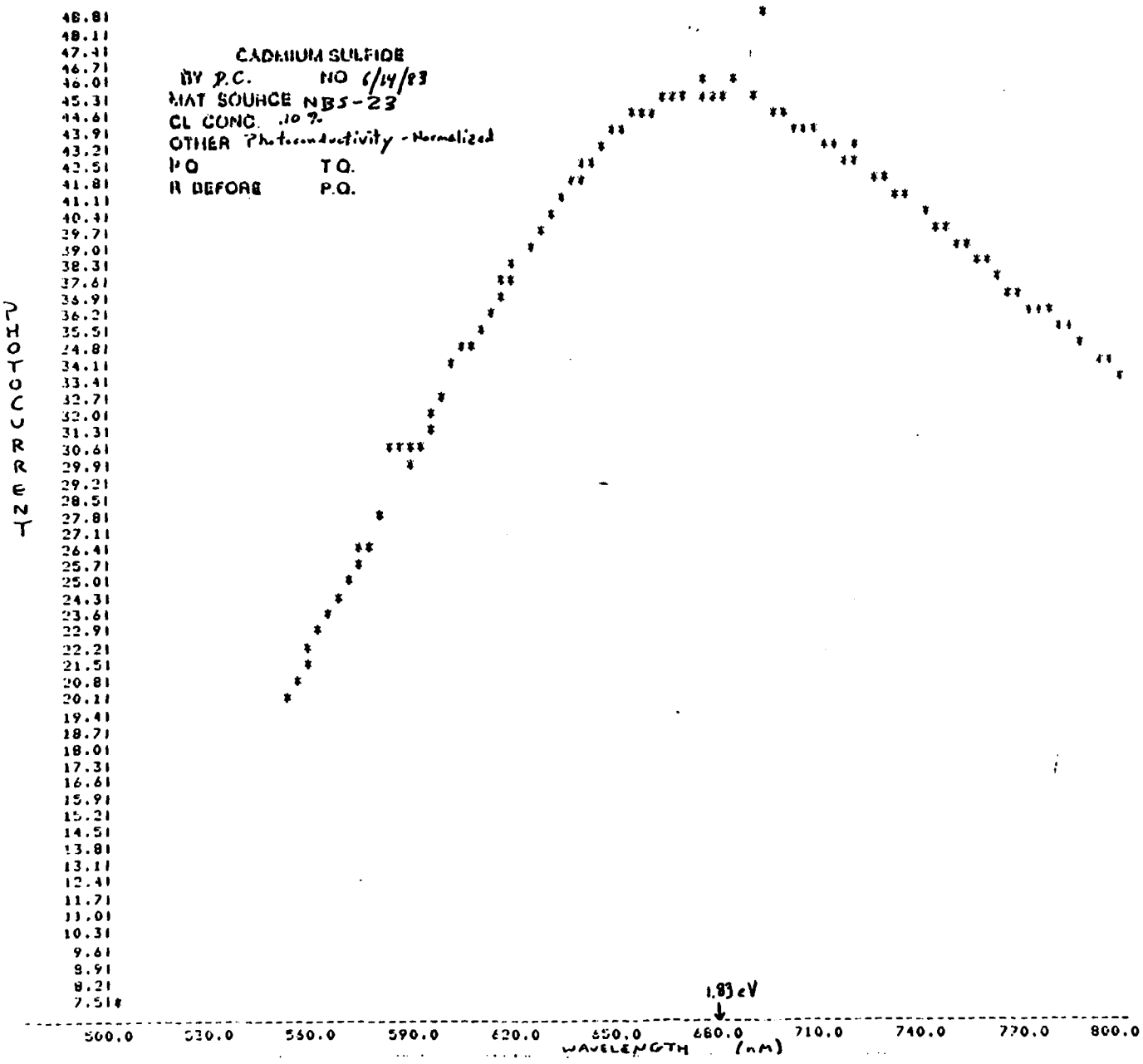
CADMIUM SULFIDE
BY P.C. NO 6/14/83
MAT SOURCE NBS-23
CL CONC .10 %
OTHER Photoconductivity - Normalized
P.O. T.O.
R BEFORE P.O.
PHOTOCURRENT
WAVELENGTH (nM)
1.83 eV
500.0
530.0
560.0
590.0
620.0
650.0
680.0
710.0
740.0
770.0
800.0

Figure 6(ii)

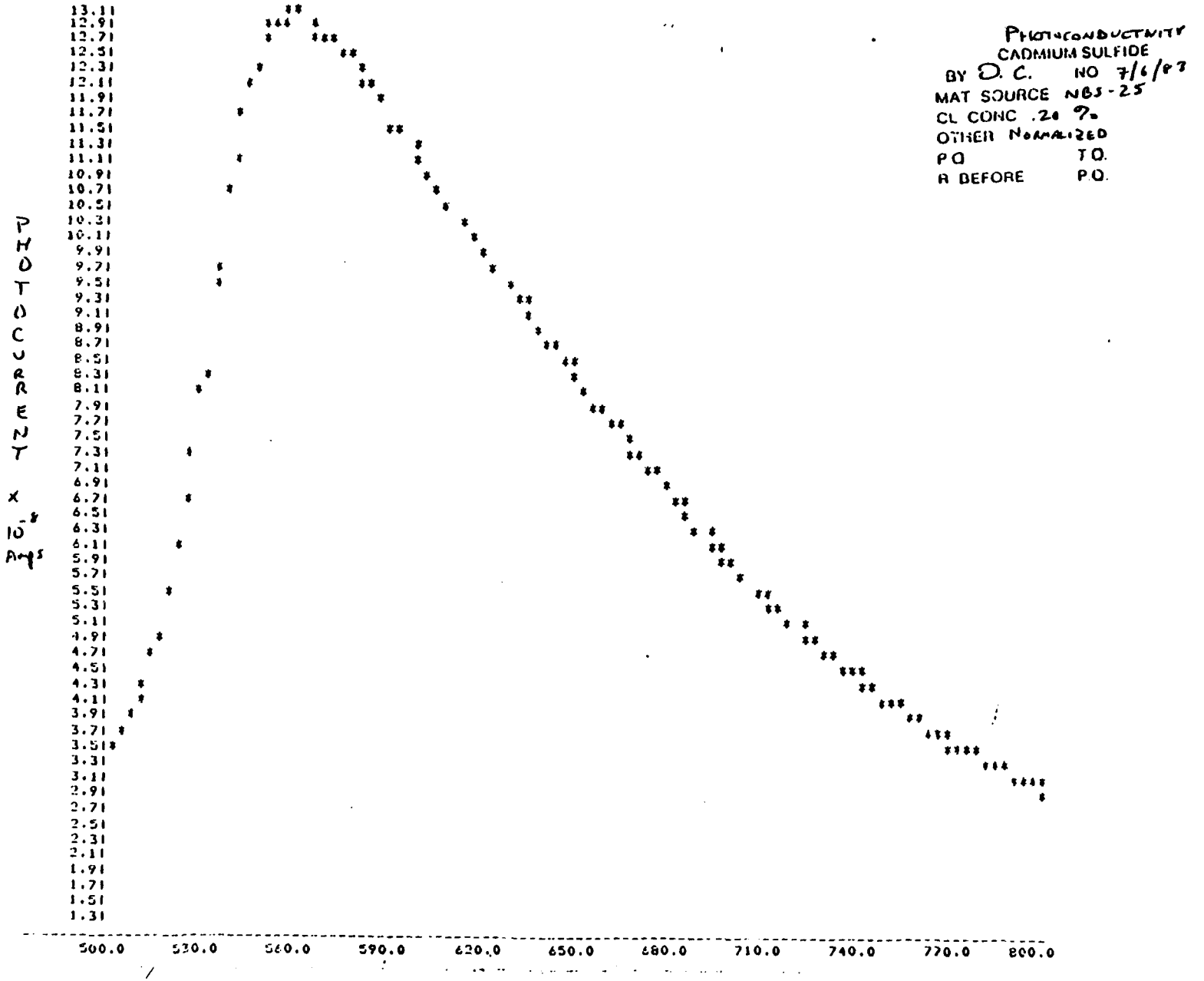
PHOTOCONDUCTIVITY
CADMIUM SULFIDE
BY D. C. NO 7/6/83
MAT SOURCE NBS-25
CL CONC .2 %
OTHER NORMALIZED
P.O. T.O.
R BEFORE P.O.
PHOTOCURRENT x 10⁻⁸ Amps
13.11
12.91
12.71
12.51
12.31
12.11
11.91
11.71
11.51
11.31
11.11
10.91
10.71
10.51
10.31
10.11
9.91
9.71
9.51
9.31
9.11
8.91
8.71
8.51
8.31
8.11
7.91
7.71
7.51
7.31
7.11
6.91
6.71
6.51
6.31
6.11
5.91
5.71
5.51
5.31
5.11
4.91
4.71
4.51
4.31
4.11
3.91
3.71
3.51
3.31
3.11
2.91
2.71
2.51
2.31
2.11
1.91
1.71
1.51
1.31
500.0
530.0
560.0
590.0
620.0
650.0
680.0
710.0
740.0
770.0
800.0

Figure 6(iii)

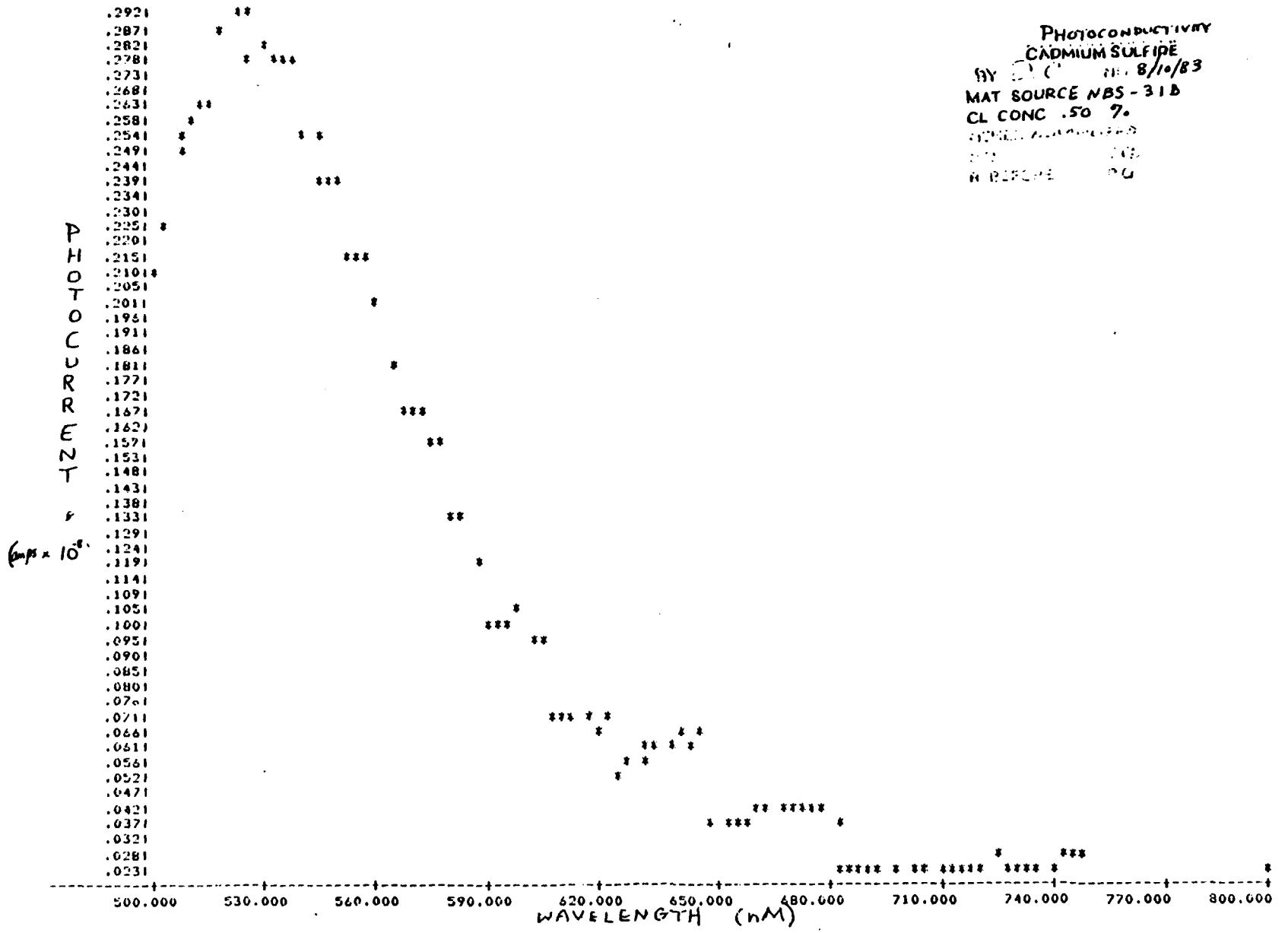
PHOTOCONDUCTIVITY
CADMIUM SULFIDE
BY
8/10/83
MAT SOURCE NBS-31B
CL CONC .50 %
PHOTOCURRENT
(amps x 10⁻⁹)
.2921
.2871
.2821
.2781
.2731
.2681
.2631
.2581
.2541
.2491
.2441
.2391
.2341
.2301
.2251
.2201
.2151
.2101
.2051
.2011
.1961
.1911
.1861
.1811
.1771
.1721
.1671
.1621
.1571
.1531
.1481
.1431
.1381
.1331
.1291
.1241
.1191
.1141
.1091
.1051
.1001
.0951
.0901
.0851
.0801
.0761
.0711
.0661
.0611
.0561
.0521
.0471
.0421
.0371
.0321
.0281
.0231
500.000
530.000
560.000
590.000
620.000
650.000
680.000
710.000
740.000
770.000
800.000
WAVELENGTH (nM)

Figure 6(iv)

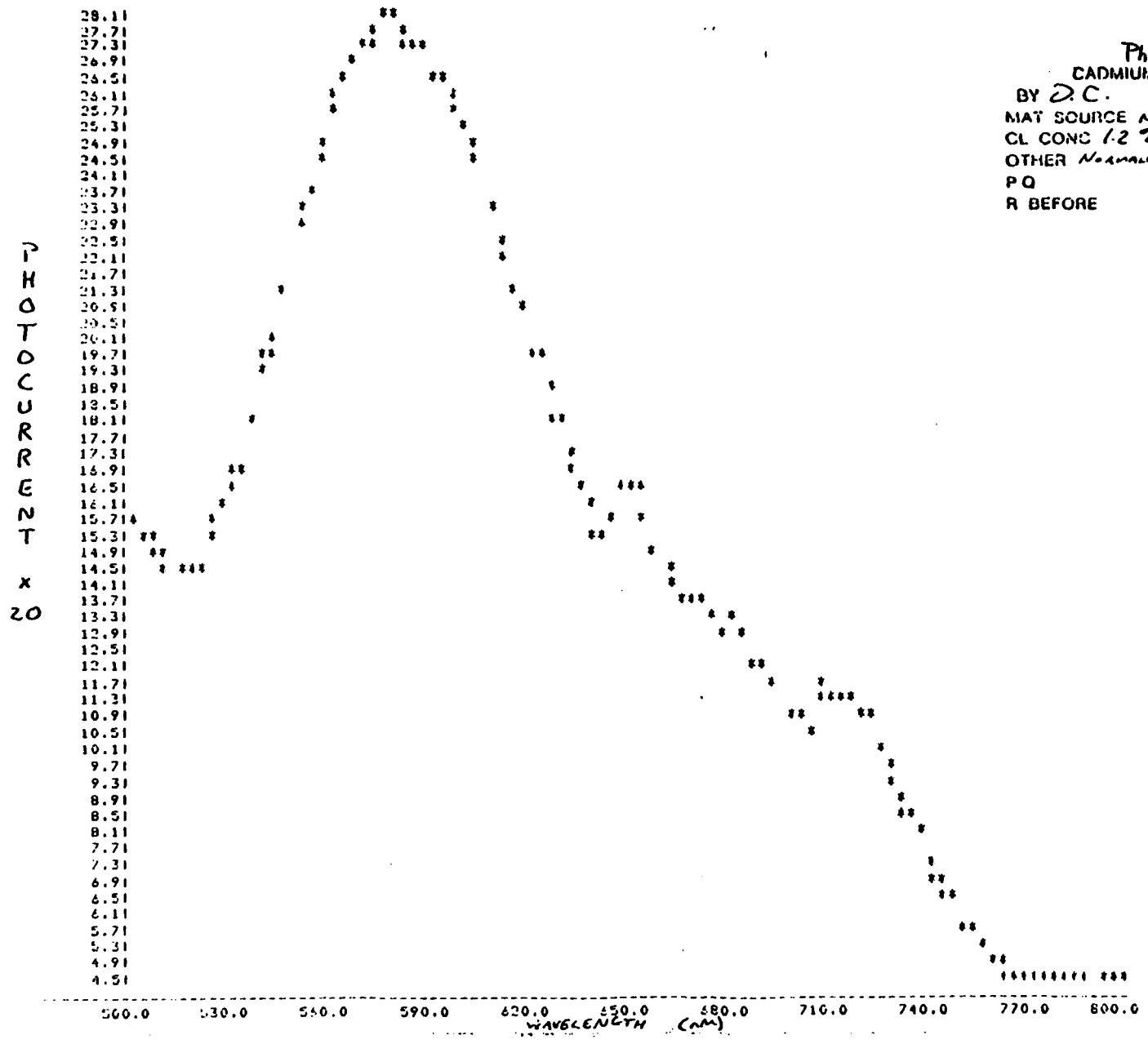
Photoconduct.
CADMIUM SULFIDE
BY D.C. NO 9/1/83
MAT SOURCE NBS-31C
CL CONC 1.2 %
OTHER NO ANNEED
P.Q T.Q.
R BEFORE P.Q.
PHOTOCURRENT x 20
WAVELENGTH (nm)
500.0
530.0
560.0
590.0
620.0
650.0
680.0
710.0
740.0
770.0
800.0

Figure 6 (v)

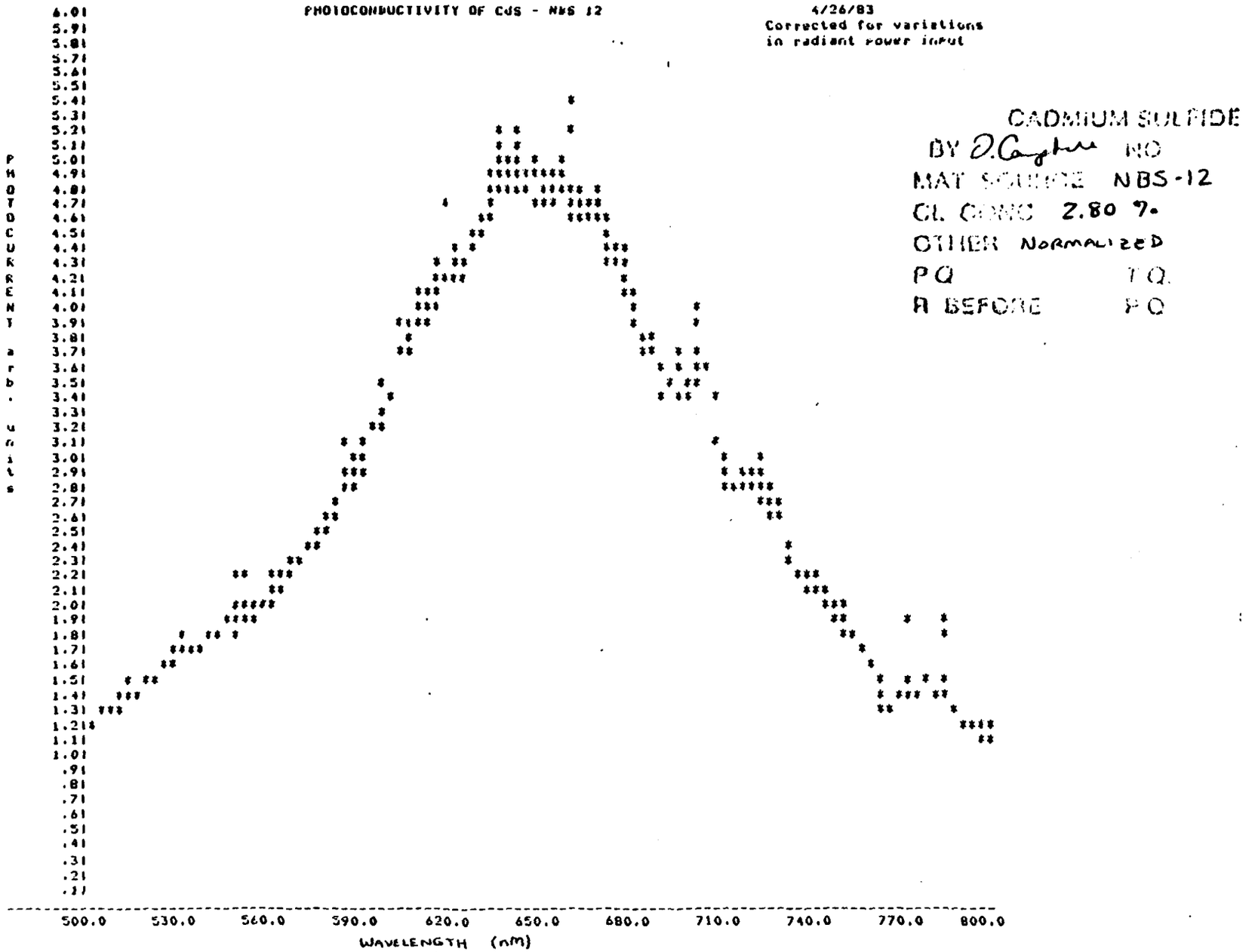
PHOTOCONDUCTIVITY OF CdS - NBS 12
4/26/83
Corrected for variations
in radiant power input
CADMIUM SULFIDE
BY D. Caplan NO
MAT SOURCE NBS-12
CL CONC 2.80 %
OTHER NORMALIZED
PQ TQ
A BEFORE PQ
PHOTOCURRENT arb. units
6.01
5.91
5.81
5.71
5.61
5.51
5.41
5.31
5.21
5.11
5.01
4.91
4.81
4.71
4.61
4.51
4.41
4.31
4.21
4.11
4.01
3.91
3.81
3.71
3.61
3.51
3.41
3.31
3.21
3.11
3.01
2.91
2.81
2.71
2.61
2.51
2.41
2.31
2.21
2.11
2.01
1.91
1.81
1.71
1.61
1.51
1.41
1.31
1.21
1.11
1.01
.91
.81
.71
.61
.51
.41
.31
.21
.11
500.0
530.0
560.0
590.0
620.0
650.0
680.0
710.0
740.0
770.0
800.0
WAVELENGTH (nM)

Figure 6(vi)

CADMIUM SULFIDE

PHOTOCONDUCTIVITY vs Cl CONTENT

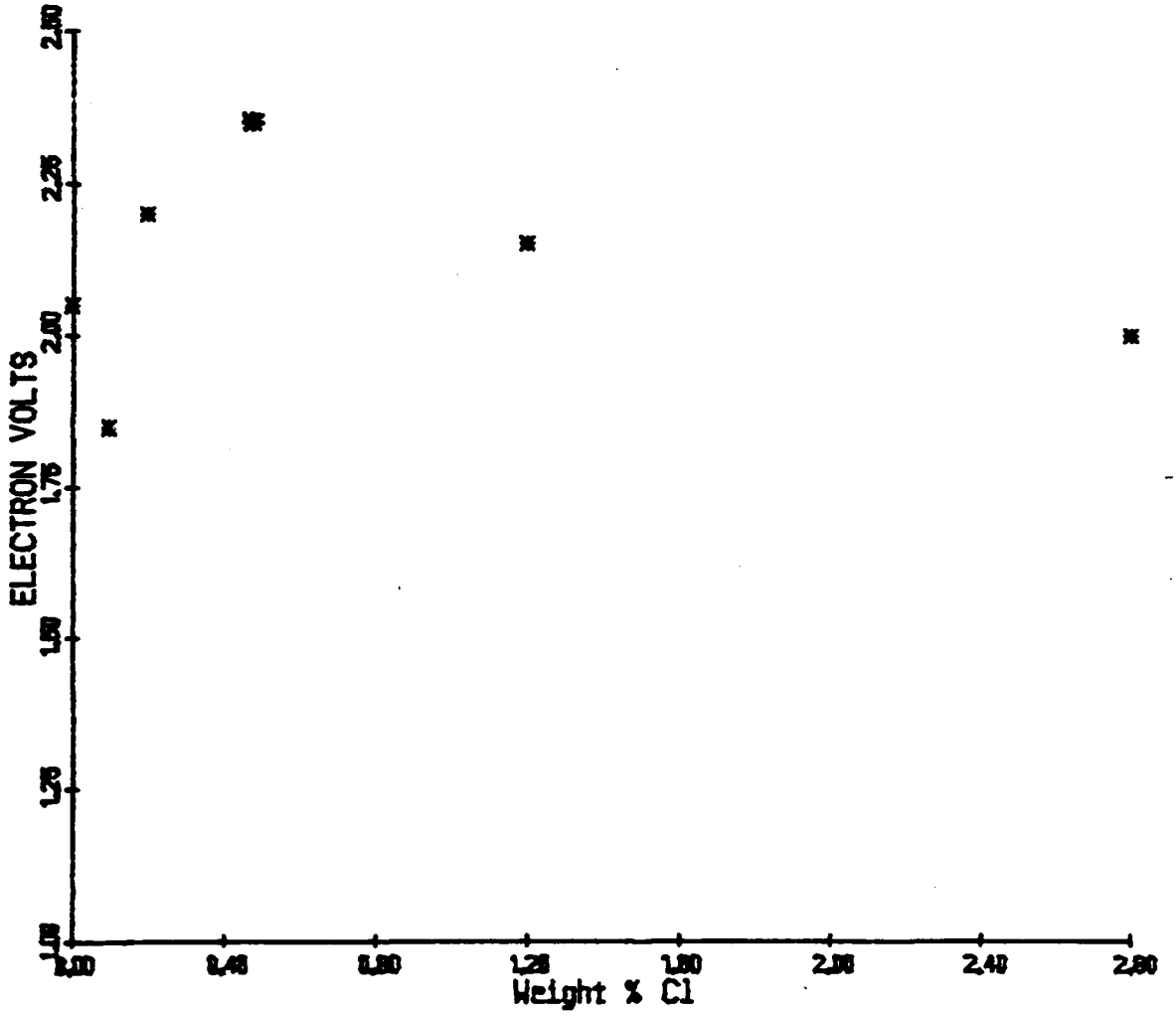

FIG. 7

SPECTRAL RESPONSE OF PHOTOCONDUCTIVITY
PRESSURE-QUENCHED CdS

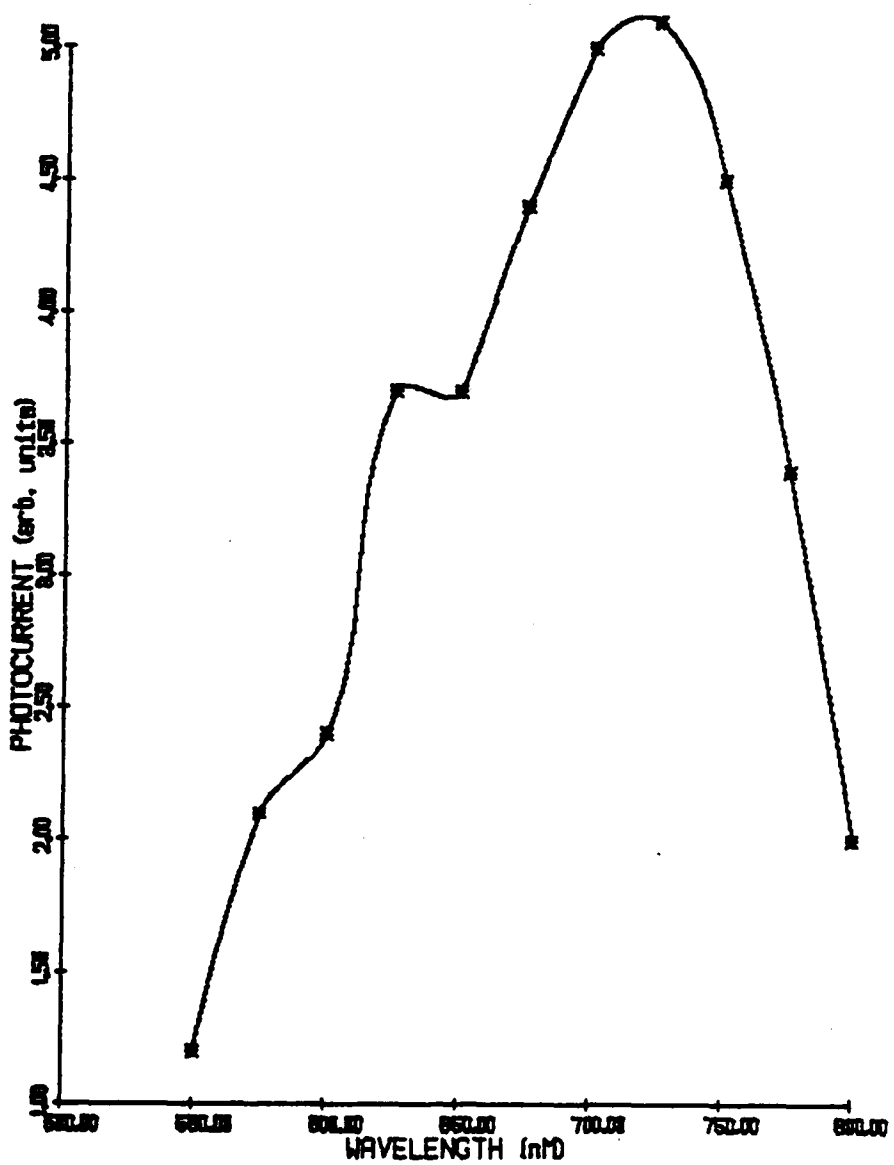

SPECTRAL RESPONSE OF PHOTOCONDUCTIVITY
PRESSURE-QUENCHED CdS

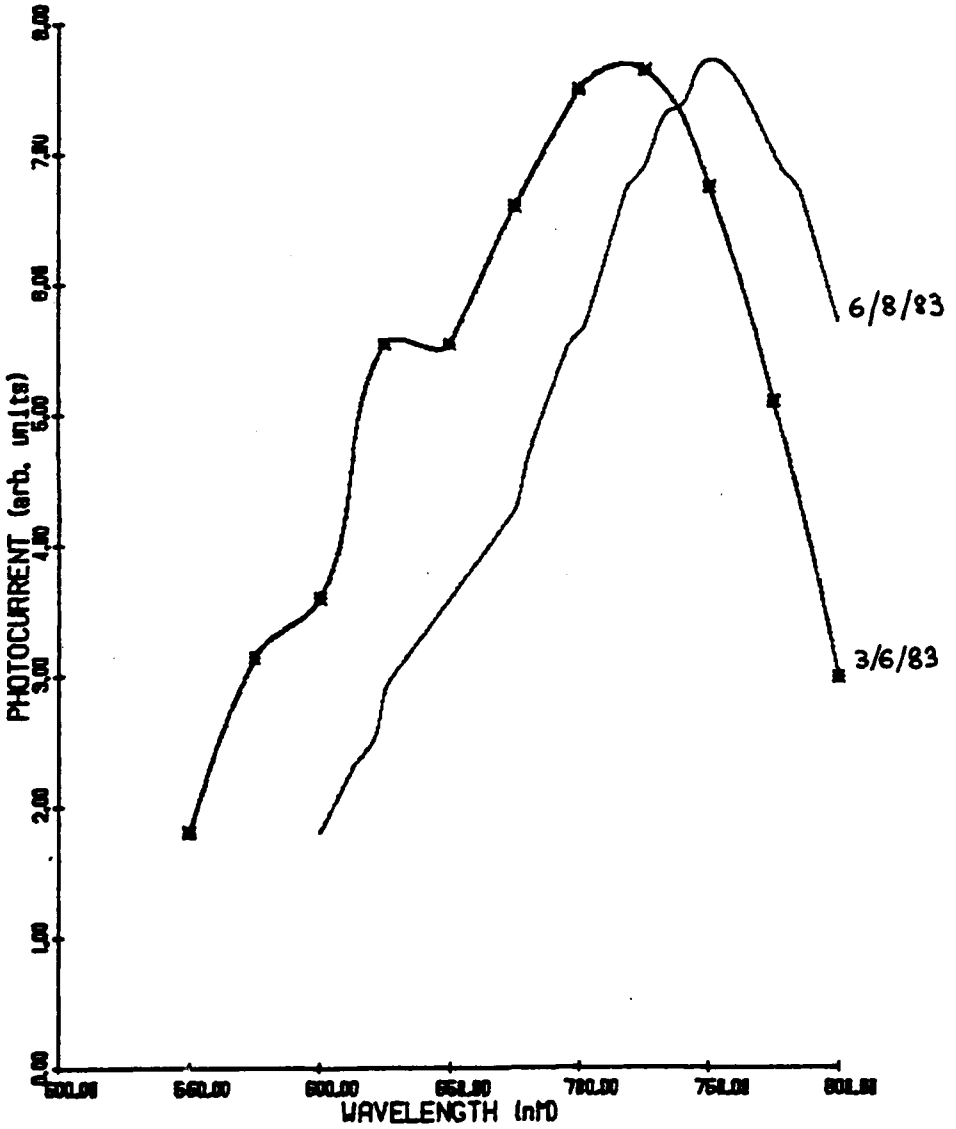

Figure 9

Presented at AIRAPT (High Pressure Conference) at SUNY at Albany, August 1983.

ANOMALOUS PROPERTIES OF PRESSURE QUENCHED CdS

R. K. MacCrone
Materials Engineering Department
Rensselaer Polytechnic Institute
Troy, New York 12181

C. G. Homan
Watervliet Arsenal
Watervliet, New York 12189

ABSTRACT

The large diamagnetism observed in pressure quenched CdS is accompanied by other physical property changes. We here describe some observations of the relation between dielectric constant, the dc conductivity and the microwave inductance of active samples. These results provide further support for high temperature superconductivity.

The extrinsic doping and defects in the active starting material are also discussed.

INTRODUCTION

The two most well known characteristics of the super-conducting state are those of zero resistance and flux exclusion, (Meissner diamagnetism). Ever since our first report of Meissner sized diamagnetism in pressure quenched CdS (1), (2), (3) we have sought to demonstrate zero resistance also in the pressure quenched CdS as a definitive test for the existence of superconductivity in our specimens. This we have not been able to do because, in principle we believe, the inhomogenity of our specimen (the specimens consist of a retained cubic phase comprising about 10% by volume in a wurzite matrix) preclude the realization of zero resistance in the absence of percolation.

However, there are observations other than zero dc resistance measurements which together with the diamagnetism provide evidence for the existence of an ordered state, very similar, if not

identical, to the superconductive state. Our experimental ploy has been to look for electrical and electro-magnetic changes at the same temperature or at the same applied magnetic field at which the diamagnetism disappears. Taking this latter to be indicative of the superconductive → normal transition, the quantity in question should change in a predictable direction. In many cases, the diamagnetic measurement has been made simultaneously on the same specimen.

The observations we present and discuss are:

(i) ac Capacitance and loss as a function of applied magnetic field at 77K
(ii) dc Resistance as a function of applied magnetic field at 77K
(iii) ac Capacitance and loss as a function of temperature at a constant magnetic field.

These measurements were made at the same time that magnetic measurements showed the disappearance of large diamagnetism.

Superconducting electrons are purely inductive, a less well known characteristic first pointed out by Pippard, and this feature is perhaps as characteristic as the Meissner effect itself. We report here observations of abrupt inductance changes in our pressure quenched specimens brought about by increasing magnetic fields or by increasing temperatures. These observations alone are very suggestive of the superconducting state. In addition, the values of the magnetic field and the temperature at which these inductance changes take place are close to those at which the diamagnetism disappears and where correlated capacitance, loss and resistance shifts also take place.

All these results can be explained on the assumption that a state, very similar, if not identical to the well known superconductive state, is present in our pressure quenched samples.

However, the state in the pressure quenched material does differ from the usual superconductive state in one important way: reversibility of behavior on temperature or magnetic excursions is seldom obtained. Often the effects and the diamagnetism are observed only once, or at most, a few times in any one sample. This aspect is different from the materials problem: that of obtaining suitable starting powder which will show these unusual behaviors on pressure quenching. We will return in detail to these apsects.

EXPERIMENTAL METHODS

The experimental techniques of preparing samples and magnetic

measurements have been well documented in previous publications (1,2,3), and will not be described here.

The ac dielectric response and the dc resistance were measured in a suitable holder which enabled the magnetisation of the specimen to be simultaneously measured as a function of both temperature and magnetic field.

The microwave inductance measurements were carried out in a homemade conventional spectrometer, operating in a dispersion mode with provisions made for measuring the incident power and the resonant frequency of the cavity. The derivative with respect to magnetic field of the reflected power was also measured. The temperature of the specimen could be varied using a Helitran system.

EXPERIMENTAL RESULTS

(i) ac Capacitance and Loss as a Function of Magnetic Field at 77K.[4]

The capacitance and loss of a pressure quenched specimen were measured; at the same time the magnetic susceptibility was monitored, the specimen being in a specially constructed holder, (details can be found in Ref. 4). The results are shown in Fig. 1a,b,c.

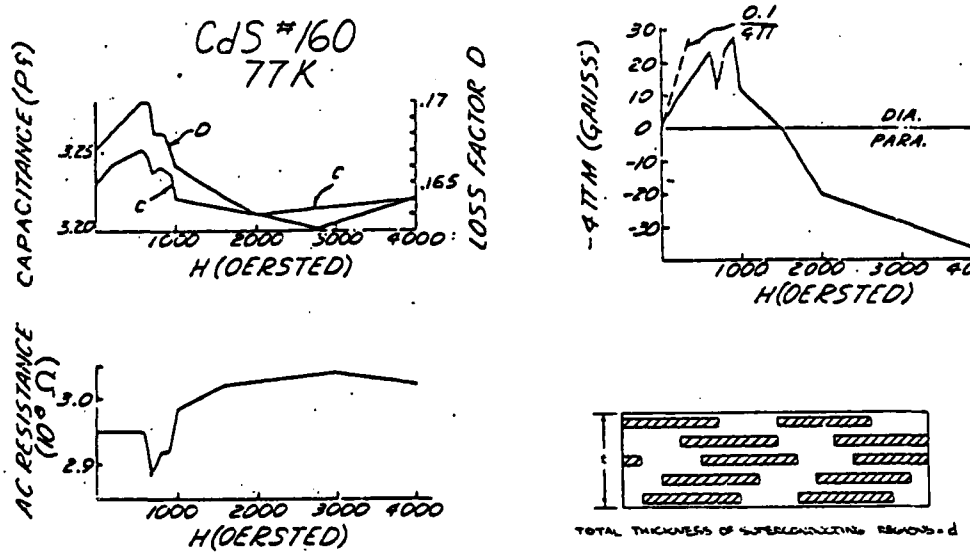

Fig. 1a,b,c. The simultaneously measured capacitance, ac resistance, and magnetization of a pressure quenched specimen of CdS at 77K.

The gross features of the observations are the diamagnetism at low fields collapsing at magnetic fields of around 1 kOe, while at the same time the capacitance and loss decrease quite strongly. Once the diamagnetism has been destroyed and the specimen driven into the paramagnetic state (a relationship not understood) the capacitance and loss become virtually independent of magnetic field.

Rather sharp electrical changes are taking place as the diamagnetism disappears. If the latter is taken as evidence for the quenching of super-conductivity, then the electrical changes are the electrical manifestation of the same process. On the basis of the morphological one dimensional sketch in the inset of Fig. 1, simple lamellar calculations show that

$$\frac{\Delta c}{c} = \frac{d}{t-d} \quad \therefore \quad \frac{\Delta R}{R} = \frac{d}{t}$$

from which the volume fraction of specimen that was superconducting can be estimated. t values turn out to 2 - 9%. These estimates can be compared with estimates based on the diamagnetism, whose value is ∿5%. It is interesting to compare these estimates with the volume fraction of retained cubic NaCl phase determined metallographically, which is also ∿ 10%.

(ii) <u>dc Resistance as a Function of Applied Magnetic Field at 77K.</u>[4]

Similarly, dc measurements were carried out under the same conditions as above, while again measuring the magnetization at the same time.

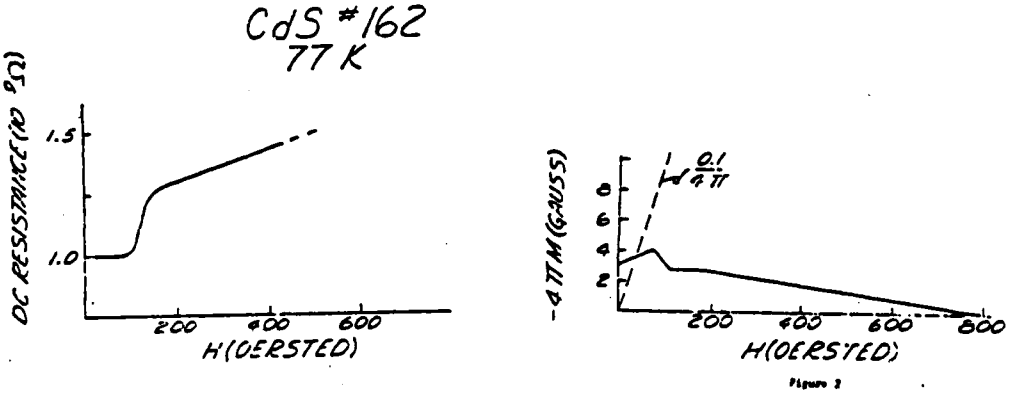

Fig. 2a,b. The simultaneously measured dc resistance and magnetization at 77K. (Same specimen as Fig. 1.)

The results are shown in Fig. 2, which give rise to the same orders-of-mangitude as in (i). For further details, Ref. 4 should be consulted.

(iii) ac Capacitance and Loss as a Function of Temperature at Constant Magnetic Field.

After pressure quenching and cooling down to 77K, the ac capacitance and loss were measured as a function of temperature. At the same time, the magnetization was monitored. The results are shown in Fig. 3, and indicate that a 2nd order transition take place at 210K as the specimen is warmed up. Such lambda point

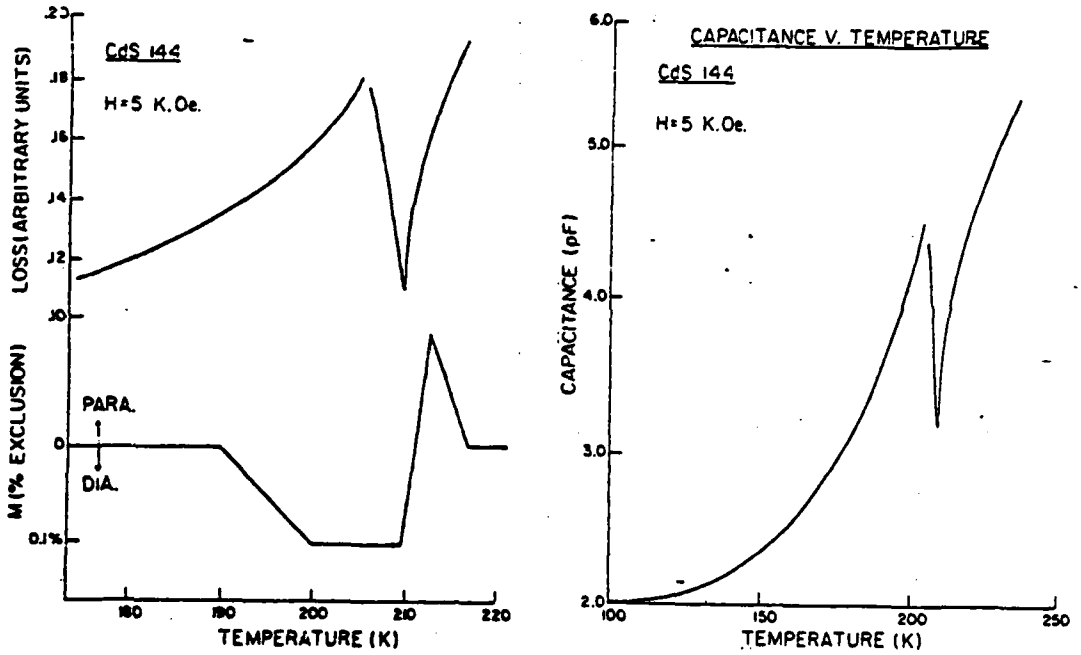

Fig. 3a,b,c. The simultaneously measured capacitance, loss, and magnetization of a pressure quenched Cds specimen as a function of temperature.

behavior in the dielectric constant are characteristic of order-disorder phase transitions (e.g., at the ferro-electric Curie point) and structural transitions (solid-solid, solid liquid)[5]. These results establish an order-disorder transition accompanied by the disappearance of large anomalous diamagnetism in the same specimen at ~200K.

We have other results pertaining to this temperature dependence of the anomalous effects. In Fig. 4 we show the diamagnetism,

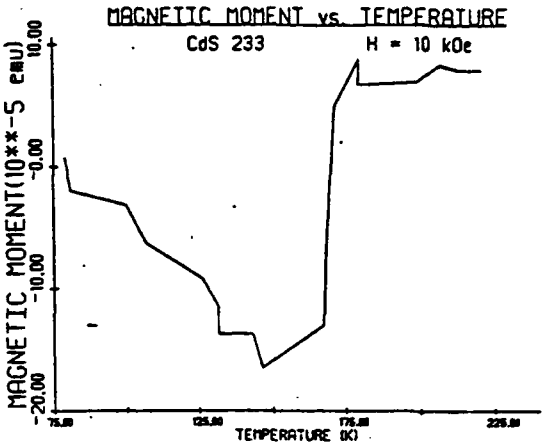

Fig. 4. The (dia-)magnetic moment of a pressure quenched specimen as a function of temperature.

at fixed field, as a function of temperature in one specimen, and a series of lambda points in the dielectric response in another sample, Fig. 5. (In these cases, simultaneous measurements were not carried out.)

From the measurements of this section we conclude that the anomalous diamagnetism can be destroyed with temperature (ascribed to some electronic state akin to superconductivity) and at the same temperature the dielectric response displays a lambda point response (not necessarily ascribed to the electronic state itself, but certainly intimately involved in some way). The data of Fig. 3 indicates that each lambda implies a diamagnetic drop in the magnetization, and vice-versa.

We note the transition temperatures T(1) = 155K, T(2) = 160K and T(3) = 195K.

Microwave Measurements

The inductive nature of superconducting electrons was first pointed out by Pippard, who showed that under the action of an alternating field their motion was inductive in character, with a

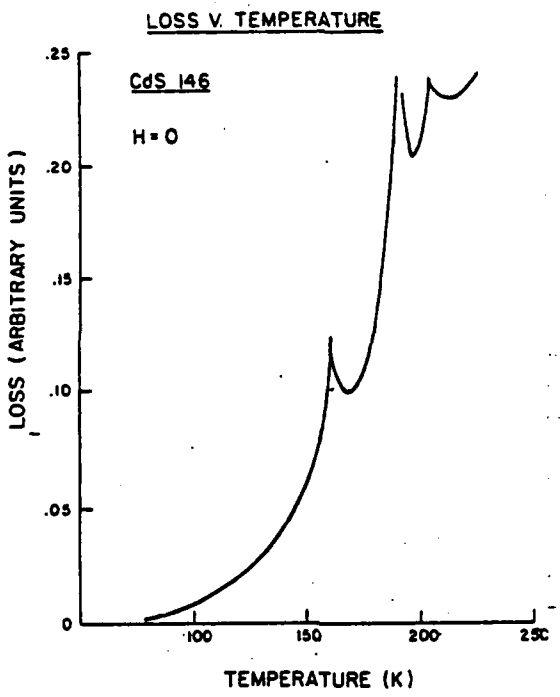

Fig. 5. The dielectric loss as a function of temperature of a pressure quenched specimen.

inductance $\frac{m}{ne}$. The classical argument is as follows:

For a sinusoidal electrical field $E_0 \sin\omega t$, the equation of motion is

$$-eE_0 \sin\omega t = m\ddot{x}.$$

Since $j = ne\dot{x}$, $\ddot{x} = \dot{j}/ne$. Substituting in the defining equation for inductance

$$E \sin\omega t = L\dot{j}$$

we find $L = m/ne^2$.

The inductive character of superconducting electrons has, for example, been used by Muller et al[6] to study the onset of the superconductivity in small grains of aluminum separated by this oxide. This technique is both contactless and samples the whole volume of the sample provided the normal electrical conductivity does not limit the penetration of the microwaves, which we believe to be case here.

Using electronic counters, the resonant frequency of the cavity-and-specimen can be used as a sensitive measure of the inductance. For a parallel coupling of cavity and specimen, the resonance frequency would be expected to go down as the specimen is driven normal by increasing temperature or by increasing magnetic field.

(iv) Microwave Inductance Shift as a Function of Applied Magnetic Field at 150K.

In Fig. 6 we show the frequency of the cavity-and-(pressure quenched) specimen as a function of applied field at 150K. At H = ∿ 1000 Oe there is a very marked frequency shift. At the same time the derivative of the power absorption was bell shaped, whose integral, the power absorbed, is also shown. At the same magnetic field that the inductance of the specimen tends towards free space,

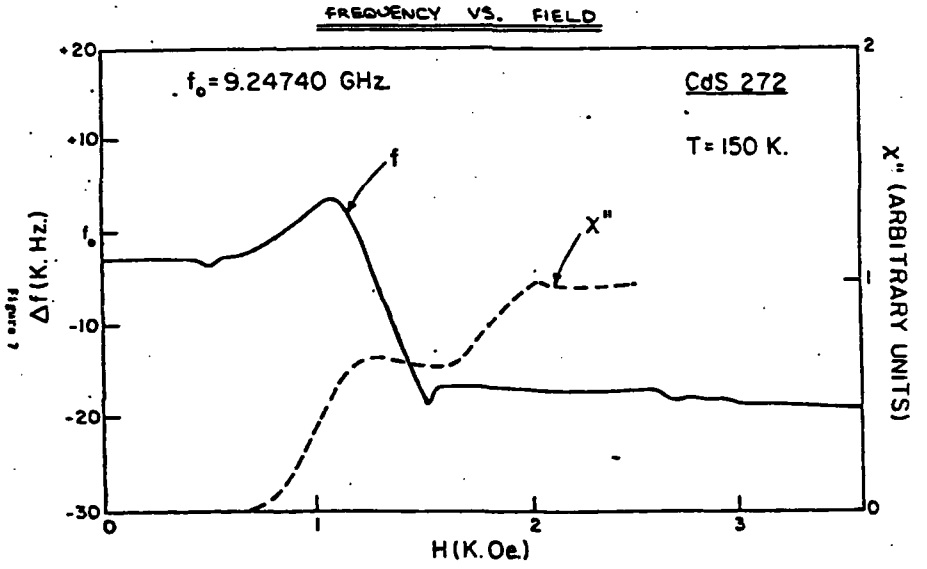

Fig. 6. The frequency and loss of the microwave cavity containing a specimen of pressure quenched CdS as a function of magnetic field.

the loss in the cavity increases. This latter is again naturally covered by the "superconductivity" hypothesis: as the superconducting electrons go normal, the number of normal electrons, to which the loss is due, goes up. Thus the loss in the cavity will likewise go up. This behavior is similar to the observations of Muller et al. [On returning the field to zero several times, and sweeping up this particular observation was repeated several times].

We note again that the magnetic field at which the transition occurs in the experiment is close to the magnetic field at which the changes in capacitance occur, Fig. 1a, and that the temperature of measurement is slightly below T(2) = 155K.

(v) Microwave Inductance Shift as a Function of Temperature.

In Fig. 7, we show the resonant frequency in zero applied field of the cavity and specimen as a function of temperature. On the generally decreasing background (caused by the increase in temperature and consequently increasing physical dimensions of the cavity) several sharp drops are observed, those at T = 100K and T = 150K being the most pronounced. These inductance changes we

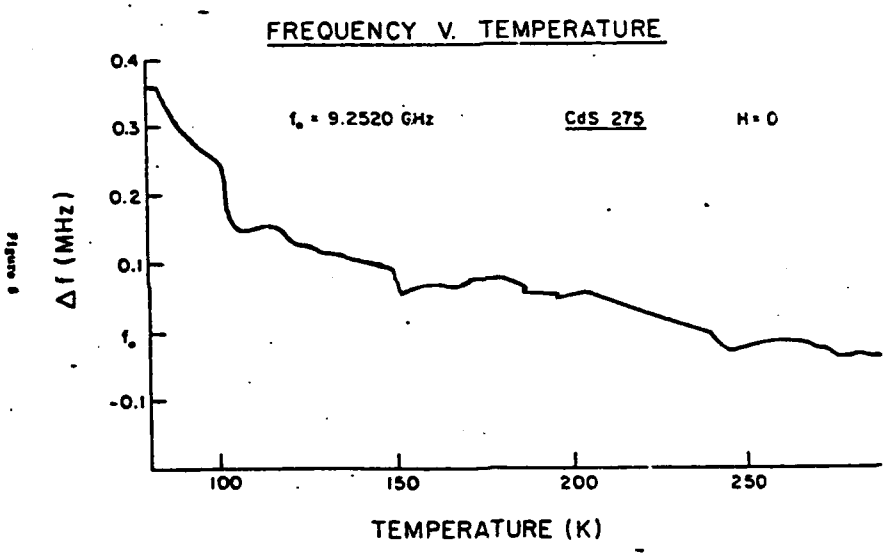

Fig. 7. The frequency of the microwave cavity containing a specimen of pressure quenched CdS as a function of temperature.

again suggest are due to superconducting to normal transitions. The temperature at which one of these sharp drops in frequency occurs is that at which lambda point behavior in the dielectric response is observed. This coincidence establishes a phase transition with the disappearance of inductance, ascribed again to superconducting electrons.

We were not able to detect changes in the derivative of the power absorption here. Whatever changes took place in this component were too small and/or spread out to be detectable in the noise at high gain. This negative result is however very important: using a Varian "strong pitch" sample our spectrometer gives a very

large signal of the derivative, but we can detect no frequency shift of the cavity. If some sort of magnetic resonance effect were involved, an observable frequency shift implies an even more easily observable derivative signal. Thus we believe no resonance phenomena are associated with the frequency shifts, and that their origin is due rather to superconducting electrons.

EVIDENCE FOR SUPERCONDUCTIVITY

In summary, our evidence for superconductivity, on some other but similar state, is based on the following series of observations:

a) large diamagnetism of Meissner proportions which can be quenched by an increasing magnetic field or by increasing temperature.
b) at the magnetic field that quenching occurs of the diamagnetism, ac and dc transport measurements on the same specimen indicate that some regions of the specimen become very much more resistive. One such possibility is, of course, from zero to some finite value.
c) a large microwave inductance (not of paramagnetic origin) which can be quenched by an increasing magnetic field or by increasing temperature.
d) at the magnetic field that quenching occurs of the microwave inductance (the specimen inductance shifts toward that of free space) the microwave loss increases. This is compatible with superconducting regions in the specimen going normal. Any increase in resistance from a finite value will <u>decrease</u> the loss, our suggestion is that the increased loss arises from an increased number of normal electrons.
e) capacitive lambda points, indicating, we believe, structural second order phase transitions at the same temperatures that the anomalously large diamagnetism disappears and microwave inductance shifts towards free space take place. Both the latter are properties of superconducting electrons, while the former establishes that a order-disorder phase transition of some sort is involved.

STARTING MATERIAL

This whole subject has been plagued by two very severe problems. One is the "transient" nature of the supposed superconducting effects, which we believe arise from the fact that they occur in a metastable phase, and some indications of the irreversible transition temperatures of this phase may be obtained from Figs. 3, 4 and 5.

The other difficulty concerns the preparation of suitable starting material. In this connection we show Fig. 8 reproduced

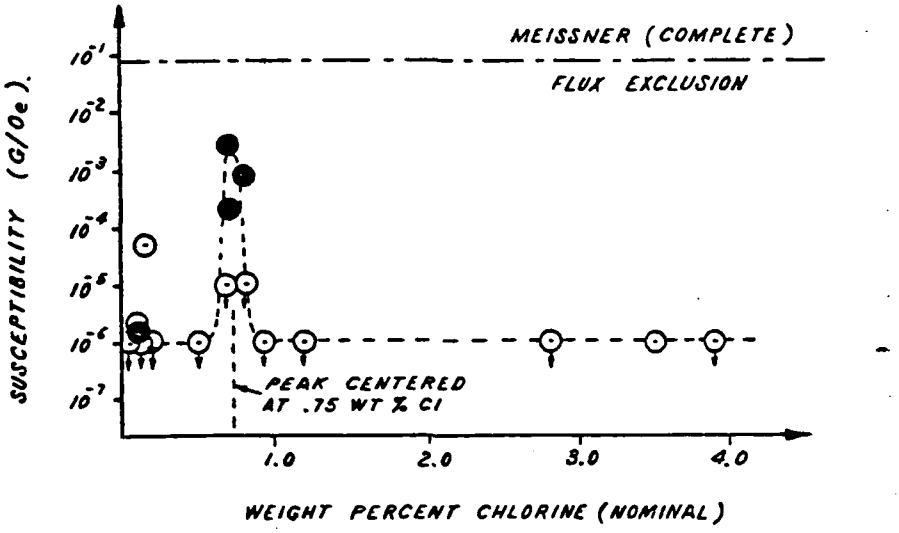

Fig. 8. The absolute susceptibility observed as a function of chlorine concentration of pressure quenched CdS.

from an extensive discussion of this subject.[7] This diagram shows the magnetization, regardless of sign, of all our specimens to date as a function of chlorine concentration. As can be seen, there is only a very narrow window of material, with chlorine content centered around 0.7 wt%, in which the phenomena in question are observed to take place after pressure quenching. Unless the chlorine concentration is within this relatively narrow range, no anomalous behavior will be observed, and this explains why our data has not been reproduced at this time. We note that obtaining the data of Fig. 8 has been no trivial matter, and that the production of starting material of suitable chlorine content even less so. The details are given in Ref. 7.

ACKNOWLEDGMENTS

The work described in this paper covers several years effort. We acknowledge the interaction and collaboration in various ways with E. Brown, D. Kendall, P. Cote, W. Moffatt, S. Block, G. Piermarini, S. Bilodeau, K. Laojindapun with financial support from the Benet Laboratory, ARRADCOM, DAAA-22-80-C-0256, the Air

Force Office of Scientific Research, AFOSR-79-0216, and the Office of Naval Research, N00014-80-C-0929, all with much appreciation.

REFERENCES

1. E. Brown, C. G. Homan and R. K. MacCrone, Phys. Rev. Lett. 45, 478 (1980).
2. C. G. Homan and D. P. Kendall, Bull. Am. Phys. Soc. 24, 316 (1979). Details are presented in Benet Weapons, Lab Report No. ARLCB-TR-79-004, available for NTIS, Springfield, VA, AD No. A069-609.
3. C. G. Homan, D. P. Kendall and R. K. MacCrone, Solid State Commun, 32, 927 (1981).
4. C. G. Homan, K. Laojindapun and R. K. MacCrone, Solid State Commun, 45, No. 8, p. 733 (1983).
5. V. A. Daniels in "Dielectrics", Academic Press, NY. and H. Frohlich in "Theory of Dielectrics", Oxford University Press, NY.
6. K. A. Muller, M. Pomerantz and C. M. Knoedler, Phys. Rev. Lett. 45, No. 10, p. 832 (1980).
7. P. J. Cote, C. G. Homan, W. C. Moffatt, S. Block, G. Piermarini and R. K. MacCrone, "Magnetic Behavior of Pressure Quenched CdS Containing Cl", Phys. Rev., to be published.

Magnetic behavior of pressure-quenched CdS containing Cl

P. J. Cote, C. G. Homan, and W. C. Moffatt
Benet Weapons Laboratory, Large Caliber Weapon Systems Laboratory, U.S. Army Armament Research and Development Command, Watervliet, New York 12189

S. Block and G. P. Piermarini
National Bureau of Standards, Washington, D.C. 20234

R. K. MacCrone
Rensselaer Polytechnic Institute, Troy, New York 12181

(Received 2 May 1983)

Pressure-quenched CdS containing Cl has been shown previously to exhibit both very large diamagnetism and paramagnetism. The diamagnetism observed at 77 K approached Meissner proportion and suggested superconductinglike behavior in this material. The effect is known to depend sensitively on the Cl content of the starting material. This paper describes the results of a survey of the magnetic behavior of pressure-quenched samples prepared from CdS systematically doped with increasing amounts of Cl. The Cl-doped material was prepared in a variety of ways: from mixtures of CdS and $CdCl_2$, by precipitation from aqueous solution, and by acid doping. The differently doped starting materials were analyzed for Cl and other impurities before being pressure quenched. The magnetic susceptibilities were subsequently measured. The results of the survey indicate that the concentration of Cl required to produce specimens with anomalously large magnetism is 0.75 ± 0.10 wt. %. The technique for the preparation of such material is described.

I. INTRODUCTION

Recently, dc flux exclusion approaching Meissner proportions in pressure-quenched CdS materials at 77 K has been reported.[1] Corroboration of these results has been provided by the work of Nam *et al.*, who found strong ac diamagnetism in several samples of CdS materials that had also been rapidly pressure quenched.[2] Cuprous chloride has also displayed similar diamagnetism after being subjected to rapid temperature variations while under pressure.[3]

Several theoretical models have been proposed to explain this anomalous diamagnetic behavior including surface superconductivity,[4] pairing of holes in semiconductors,[2] finite-momentum pair binding in a one-dimensional system,[5] and an excitonic mechanism for superconductivity related to the presence of impurities.[6]

In the magnetically active CdS materials, it was also found that anomalous and very large paramagnetism occurred in some of the pressure-quenched samples.[7] The most recent work describes the simultaneous decrease of both the ac and dc electrical conductivity with the loss of flux exclusion, which supports the claim of some form of collective behavior in such materials.[8,9] Both the anomalous diamagnetism and paramagnetism were found to be metastable.[10] The magnetically active samples had a morphology of *lenticular platelets embedded in a microcrystalline matrix*[11] and contained a mixture of wurtzite (Greenockite), zinc-blende (Hawleyite), and NaCl crystal structures. The magnetic effects were also found to be dependent on sample material origin and chemistry.[7-10]

In all the previous work published by the present authors, these unusual electrical and magnetic properties were observed in samples made from a single lot of commercial high-purity CdS powders obtained from Alpha Inorganic (AI) and only after rapid pressure quenching (greater than 10^5 bar/sec) from above the well-known *wurtzite-to-NaCl phase transition* at ambient temperatures.[12] These anomalous phenomena were *never* observed in samples made from any source other than the particular lot from AI or in any samples which were slow quenched from above the high-pressure transition.

It is thus clear that the anomalous behavior depends on both the sample chemistry and pressurization parameters. Here we describe our investigation of the chemistry of the as-received materials used in the previous work and identify the critical chemistry involved in the phenomena. This chemistry was determined by the correlation of the electrical and magnetic properties with the sample impurities and dopants of both as-received and -prepared materials. We will also describe material-preparation techniques which provide samples which gave similar anomalous results after pressure quenching. Other physical properties which depend on the sample chemistry, as well as the resulting morphology, are described.

The implications of these material studies will be discussed. A tentative model relating to metastable phase decomposition (NaCl phase) will be suggested to explain the correlation between sample chemistry and morphological behavior after various pressure treatments.

II. CHEMICAL ANALYSIS OF AS-RECEIVED CdS MATERIALS

Since a qualitative analysis of the magnetically active AI and nonactive Eagle Picher (EP) materials by a spark-

emission technique did not show any appreciable difference in the metallic impurity spectrum,[10] a more comprehensive chemical analysis was performed by the National Bureau of Standards (NBS) on these materials and on other magnetically nonactive sample materials.

Initially, a qualitative evaluation by x-ray fluorescence (XRF) was made using both energy- and wavelength-dispersive spectrometers. This technique has detection limits of the order of 1–10 ppm for all elements $Z > 11$. Trace elements Cl, K, Fe, Cu, Zn, and Ge were detected near the limit of detection by XRF in the magnetically active AI material suggesting that impurity levels were of the order of 10 ppm.[1]

Both pressed starting pellets and pressure-quenched samples of the various as-received materials were further analyzed by electron-probe microanalysis with dispersive x-ray spectrometry (EDS). In general, this technique is sensitive to all elements $Z > 11$ with a limit of detection of the order of 0.1 wt.% and a sampling depth of about 1 μm. Five samples were examined on the outer surfaces or on freshly exposed fracture surfaces using the NBS theoretical-matrix frame-P procedure for rough surfaces.[13] Frame P is believed to have an error distribution within 20% relative.

Six pressure-quenched samples (three each from the AI and EP material) were metallographically cross-sectioned and analyzed, corresponding to interior and near-surface regions of the samples. Quantitative analysis of these samples were made using NBS frame-C procedures.[14] Frame-C procedures yield an error distribution such that 95% of all samples fall within 5% relative to the amount present on metallographically polished surfaces.

The metallographically mounted samples were further analyzed by an ion-microprobe analysis (IMA). This analytical technique has very high sensitivity (typically 1 ppm) for all elements of the Periodic Table.

The result of these extensive analyses were that the magnetically active AI starting powder had substantial levels of Cl impurities in addition to the trace metallic impurities reported earlier.[10] The quantitative analyses by EDS and IMA technique revealed that the Cl levels in pressure-treated and magnetically active AI materials was about 1.0 wt.% and that the Cl was distributed nonuniformly within the samples. The nonactive materials, especially the EP material, showed *no* detectable Cl contamination within the combined sensitivities of the EDS and IMA techniques. This analysis shows that Cl levels, if present, were below 0.01 wt.% in the nonmagnetic materials such as the EP materials.

Si was also detected in the pressure quenched samples from both AI and EP materials. The EDS technique indicated that Si was also distributed nonhomogeneously in the samples with an average level of 0.15 wt.% in the AI materials and 0.05 wt.% in the EP materials. Since Si was not detected in the as-received powders from these sources, we concluded that the Cl impurity contamination was critical in producing the magnetic anomalies. Si may have been introduced by either exposure to the pyrophyllite gaskets used in pressurizing the samples or from the silicone grease used to mount the samples for the magnetic measurements after pressurization before chemical analysis. This conclusion was supported by the fact that samples containing Si introduced by either means did not show magnetic anomalies when the Cl content differed significantly from the AI material.

III. PREPARATION OF Cl-DOPED CdS MATERIALS

In view of the above results, a variety of preparation techniques were used in an attempt to make suitable doped materials. Earlier differential scanning calorimetry (DSC) results had suggested that the active AI material had been prepared by a precipitation technique.[15]

A. Mixtures of CdS and $CdCl_2$ powders

Pure CdS powders (EP) were mixed with reagent-grade $CdCl_2$ powders to yield nominal Cl contents of about 1.0, 1.5, and 2.0 wt.% of the mixture. The thermal properties of these materials, both in the as-prepared and in the as-quenched condition were measured by the DSC technique described elsewhere.[15] The only peaks observed were the dehydration peak at 100°C from the hydrated $CdCl_2$ powder and the eutectic melting peak at 535°C of the mixture suggesting that the NaCl high-pressure phase was not retained after pressure quenching. None of these materials exhibited anomalous magnetism after pressure quenching.

B. Precipitation reaction

The standard procedure of producing CdS materials by precipitation from a hydrous $CdCl_2$ solution using H_2S gas was used. Small batches ($\sim$100 ml) of $CdCl_2$ solutions with starting molarities in the range 0.1–1.0M with respect to Cl were prepared. These solutions had the natural pH of solution. Precipitation of CdS materials from these solutions at ambient temperatures occurred when the insoluble CdS precipitated as H_2S gas was slowly bubbled through the solution. The CdS precipitate contained between 0.5 and 4.11 wt.% Cl varying roughly with the molarity of the starting solution. The nominal Cl and S contents were determined by an ion-chromatography method developed by NBS.[16] Ultrasonically washing the precipitate in distilled water revealed that roughly half of the Cl content was easily removed. The remaining Cl is probably incorporated in the CdS lattice.

Both pellets and pressure-quenched samples made from these materials were studied by DSC and their behavior was similar to the behavior of the AI material reported earlier.[15]

Some variability in Cl conent within each precipitate aliquot occurred suggesting that critical chemical parameters, such as the decrease in molarity as the reaction proceeds, were affecting the Cl content of these batch-produced materials.

An analysis of the various ionic species present in the aqueous solutions of $CdCl_2$ was made using equilibrium constants (K_i) in the following set of competing reactions:

$$Cd^{2+} + Cl^- \overset{K_1}{\rightleftharpoons} CdCl^+, \quad K_1 = 21.0 \tag{1}$$

$$Cd^{2+} + 2Cl^- \overset{K_2}{\rightleftharpoons} CdCl_2, \quad K_2 = 166.0 \tag{2}$$

$$Cd^{2+} + 3Cl^- \overset{K_3}{\rightleftharpoons} CdCl_3^-, \quad K_3 = 204.0 \tag{3}$$

$$Cd^{2+} + 4Cl^- \overset{K_4}{\rightleftharpoons} CdCl_4^{2-}, \quad K_4 = 7.15 \tag{4}$$

which can be expressed in the generalized form

$$Cd^{2+} + nCl^- \overset{K_n}{\rightleftharpoons} CdCl_n^{(-n+2)}, \quad K_n,\ n = 1,2,3,4\ . \tag{5}$$

The fraction α_n of a particular equilibrium species present in solution can be given as

$$\alpha_n = \frac{[CdCl_n]}{C} = K_n[Cl^-]^n \alpha_0\ ,$$

where

$$\alpha_0 = \frac{[Cd^{+2}]}{C}\ ,$$

and C is the total concentration of cadmium-containing species. Given the initial Cd^{+2} and Cd^- concentration, the equations can be solved for α_n. The results for various $CdCl_2$ molarities are shown in Fig. 1. The wide variation in the different ion species especially in the region of molarity below 0.5*M* where the magnetically active AI materials were produced is quite apparent. It is not clear which ion or combination of these ions produces the necessary complex in the precipitate which yield anomalous magnetism after pressure quenching.

A preliminary examination of the precipitated materials by transmission-electron-microscopy (TEM) and small-angle x-ray-scattering techniques showed the presence of small spherical crystallites (diam. ~50 Å) in the precipitated powders in good agreement with the results of Sato, Itoh, and Yamashita.[17]

Examination of these materials by DSC show only the eutectic melting peak associated with a mixture of $CdCl_2$ and CdS, indicating that the initial complex compound decomposed to a simple mixture upon heating; no dehydration peak was observed, which indicates that the as-precipitated powders are not a simple mixture of CdS and $CdCl_2$. These results were also obtained on the magnetically active AI starting powders.[15] Pressure-quenched samples of the precipitated powders containing Cl > 0.7 wt. % exhibited the exothermic peak associated with the transformation of the metastable NaCl high-pressure phase. Pressure-quenched samples made from powders containing less than 0.7 wt. % Cl showed a retained NaCl phase in addition to the wurtzite and zinc-blende phases by both x-ray examination and optical evidence of small platelets. The magnetic behavior of pressure-quenched samples of these materials are shown in Fig. 2 and will be discussed subsequently.

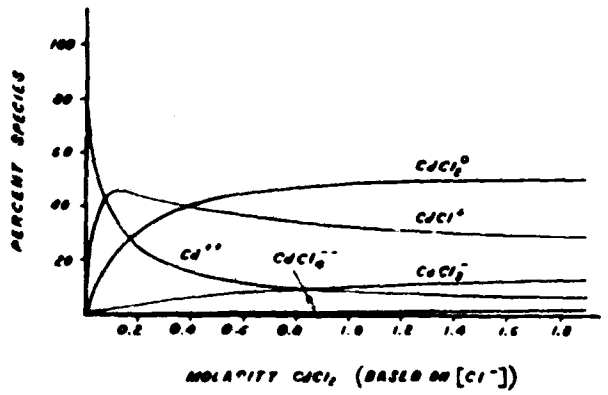

FIG. 1. Variation of ionic species present in aqueous solution of $CdCl_2$ as a function of the molarity of solution based on $[Cl^-]$ chloride-ion concentration in mole/l.

IV. ACID-DOPING TECHNIQUE

Samples of pure CdS were stirred and heated with various HCl and NaCl solutions to determine whether Cl^- could be incorporated directly into the CdS lattice. This technique produced CdS materials containing Cl levels of about 0.1 wt. %. Again about 50% of the Cl content could be removed by ultrasonically washing the powders in distilled water. It was not possible to obtain Cl contents above 0.2 wt. % by this technique.

DSC analysis of the acid-leached samples revealed no eutectic melting peak at 535 °C in the precipitate powders and a broad weak exotherm centered around 350 °C in pressure-quenched samples. This indicates retention of only a small quantity of the zinc-blende phase, characteristic of very pure CdS.[15] Metallographic examination of the samples revealed a small fraction of platelets after quenching, which suggests a retained NaCl phase in these samples which was below the sensitivity of the DSC technique.

The magnetic behavior of pressure-quenched samples made from these materials are shown in Fig. 2 and are discussed subsequently.

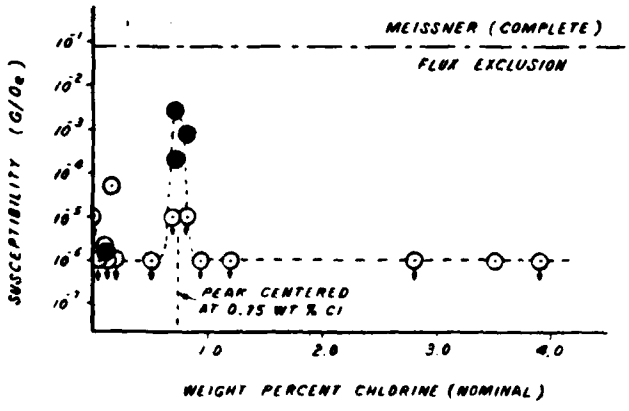

FIG. 2. Mean value of the absolute magnetic volume susceptibility from each sample lot is plotted as a function of the nominal Cl content of the lot. Solid symbols represent the mean value determined from 10 or more observations on a particular sample lot as tabulated in Table I. Of the 115 observations represented in this figure, all but nine measurements which were measured at liquid-He temperatures in either the SQUID or ac magnetometers; the rest were measured at liquid-N_2 temperatures.

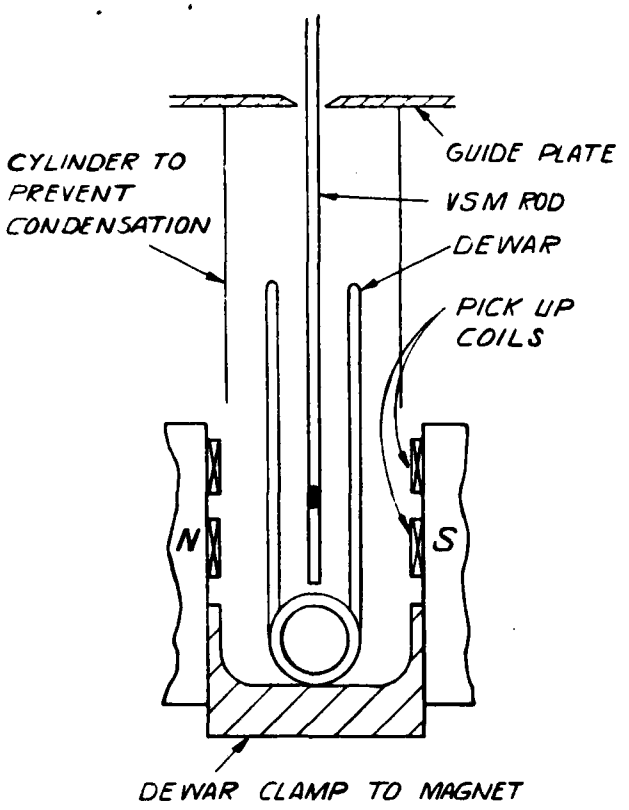

FIG. 3. Schematic of the sample chamber of the VSM. A Helitran cryogenic cooling system was used to provide the liquid-N_2 measurement temperatures.

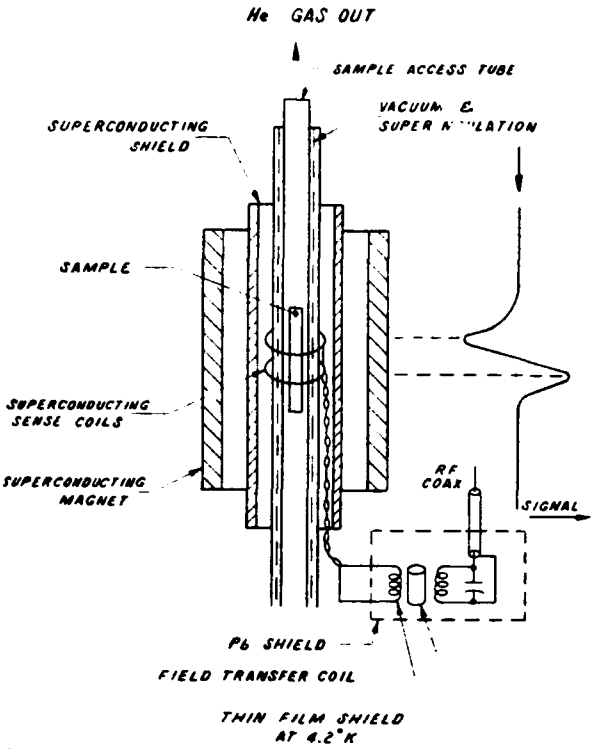

FIG. 4. Schematic of SQUID magnetometer used at liquid-He temperatures. Typical signal generated as the sample is drawn through the sense coils is shown at right.

V. MAGNETIC MEASUREMENTS

The dc magnetization as a function of magnetic field was determined by either a vibrating-sample magnetometer (VSM) or a superconducting quantum interference device (SQUID) magnetometer. The ac susceptibility was determined using the Hartshorn bridge described earlier.[11]

The VSM measurements reported here were made in a variety of sample chamber configurations. The configuration shown in Fig. 3 was used for more than half the samples tested. A modification of this basic design was used to measure the simultaneous changes in electrical conduction and magnetic moment of 17 samples reported elsewhere.[8,9] In all sample configurations, the magnetic moment was measured using field sweeps below 100 Oe/min and no systematic errors were observed.

The first nine samples measured in the VSM were mounted in a Teflon sample holder which placed the samples in a random orientation with respect to field. This random orientation was fixed for each measurement, however. Sample CdS No. 51, which was measured in the Teflon sample holder, was examined for field-orientation effects. At high field (greater than 1000 Oe) this sample exhibited large paramagnetism. By rotating the VSM vibrator about the axis of the sample rod we observed a large but reproducible variation in magnetic moment at constant field. A cursory examination of our sample geometry suggested that the maximum moment occurred when the field was oriented in the plane of the sample. All subsequent sample holders were designed to align the field with plane of the disc samples. Therefore, all subsequent samples were measured in this manner.

The SQUID magnetometer shown schematically in Fig. 4 allowed the magnitude and sign of the magnetic moment to be determined in fields up to 60 kOe at liquid-He temperatures. Both the SQUID and VSM systems were periodically calibrated using Ni and $CuSo_4 \cdot 5H_2O$ as standards. The ac bridge was calibrated using the superconducting transition in a Pb sample. The diamagnetic susceptibilities were determined from either the slope of the measured M-vs-H curves from the VSM or by direct comparison with known standards in the SQUID and ac magnetometers.

For those samples exhibiting paramagnetism in the VSM, the generally small region of low field where the samples were diamagnetic was neglected and the susceptibility was determined by forcing the intercept of the slope to pass through the origin of the M-vs-H plot. In a few cases where this analytic technique could lead to serious error in determining χ, i.e., when the diamagnetism persisted to above 100 Oe before becoming paramagnetic, the actual slope of the M-vs-H plot was calculated. Six such samples were of the latter type and are included in Table I with both their diamagnetic and paramagnetic susceptibilities. The remaining paramagnetic samples had diamagnetic regions of such small extent that it was not possible

TABLE I. Diamagnetic and paramagnetic susceptibilities of pressure-quenched Cds, containing Cl samples.

Sample lot no.	Material source	Cl (wt. %)	Method of preparation	$\lvert\chi\rvert_{mean}$	χDia^{max}	$\chi Para^{max}$	Number of observations
1	Eagle Picher (EP)	0	n.a.	$<1.0\times10^{-5}$			3
2	Alpha Inorganic (AI)[a]	0	n.a.	$<1.0\times10^{-5}$			2
3	NBS 21A	0.04	acid doped	$<1.0\times10^{-6}$			3
4	NBS 23	0.10	acid doped	$<2.0\times10^{-6}$	-2.0×10^{-6}		1
5	NBS 21	0.13	acid doped	$<1.0\times10^{-6}$			2
6	NBS 22	0.14	acid doped	1.4×10^{-6}	-5.0×10^{-6}		10
7	NBS 26	0.16	acid doped	5.3×10^{-5}	-1.6×10^{-4}		4
8	NBS 25	0.20	acid doped	$<1.0\times10^{-6}$			1
9	NBS 28	0.20	acid doped	1.0×10^{-6}	-1.0×10^{-6}		2
10	NBS 31B	0.50	precipitation	$<1.0\times10^{-6}$			1
11	NBS 5	0.68	precipitation	$<1.0\times10^{-5}$			1
12	NBS 8	0.72	precipitation	2.2×10^{-4}	-1.6×10^{-3}		14
13	AI[b]	0.72	n.a.	2.4×10^{-3}	-4.0×10^{-2}	$+1.4\times10^{-3}$	51
14	NBS 1	0.83	precipitation	7.9×10^{-4}	-7.9×10^{-3}		11
15	NBS 2	0.83	precipitation	$<1.0\times10^{-5}$			2
16	NBS 17	0.93	precipitation	$<1.0\times10^{-5}$			1
17	NBS 31C	1.2	precipitation	$<1.0\times10^{-5}$			1
18	NBS 12	2.8	precipitation	$<1.0\times10^{-5}$			3
19	NBS 20F.5-2	3.5	precipitation	$<1.0\times10^{-5}$			1
20	NBS 11	3.9	precipitation	$<1.0\times10^{-5}$			1

[a] AI stock number 20130, lot number 062778.
[b] AI stock number 20130, lot number 033072.

to determine their diamagnetic susceptibilities.

The average absolute volume susceptibilities of pressure-quenched samples from each sample lot were determined and tabulated in Table I together with source identification, Cl content, preparation technique, the maximum diamagnetic and paramagnetic susceptibilities observed, and the number of observed points.

Not included in this tabulation are the results for an additional 20 samples, which were either starting pellet samples, samples which had been slowly depressurized (less than 10^3 bar/sec) from above the NaCl transition pressure, or samples which had been rapidly quenched from below this transition. These samples were made from various Cl-containing materials described above and none exhibited any detectable anomalous susceptibility in the SQUID or VSM systems.

Only pressure-quenched samples from the AI source containing 0.72 wt. % Cl exhibited both diamagnetism and paramagnetism. The IMA showed that the paramagnetic and ferromagnetic impurity elements in this material were below 20 ppm by weight and cannot account for the large paramagnetic susceptibilities observed here. In addition, the detailed behavior of the paramagnetism observed[7,10] precludes the possibility of sample contamination as being the cause of this anomalous behavior. Of the 51 measurements made on this material we observed anomalous paramagnetism 16 times.

The mean value of $|\chi_v|$ for each sample material lot is plotted as a function of Cl content in Fig. 2. The curve shown is a reasonable fit to these values neglecting the single point at 0.16 wt. % Cl whose value was 5.3×10^{-5} G/Oe. The data shown in Fig. 2 was obtained from 115 observations on 109 different samples. The nominal Cl content is the average Cl determined from several analyses of each sample material lot. The Cl uncertainty was approximately 10% relative in the acid-doped material and approximately 20% relative in the precipitated material.

The mean diamagnetic susceptibility of all observations on sample materials, excluding the magnetically active NBS 1 (sample 14), NBS 8 (sample 12), and AI Lot-033072 (sample 13) materials, was calculated. A mean diamagnetic volume susceptibility of the order of 1×10^{-5} G/Oe was determined using 39 data points which is in good agreement with the volume susceptibility calculated from handbook values of the diamagnetic susceptibility and the mass ($\sim$15 mg) of the samples.

VI. PLATELET VOLUME MEASUREMENTS

Quantitative metallography often serves as a sensitive guide to the physical processes that material specimens have undergone and is an especially useful adjunct technique in studying the morphology of samples of different chemical compositions which may have a profound effect on the physical behavior observed.

Fast- and slow-quenched EP samples appeared to be nearly 100% wurtzite phase after quenching. The small amount of zinc-blende phase reported earlier in the x-ray and DSC analysis[15] could not be distinguished by this technique. In both cases, the crystallites were pancake shaped with the axis of rotational symmetry along the load axis. The diameter of the crystallites after fast quenching was about 70 μm and the thickness was about 20 μm. After slow quenching these values became 120 and 30 μm, respectively. It is important to note that over 4 orders of magnitude, change in the depressurization rate

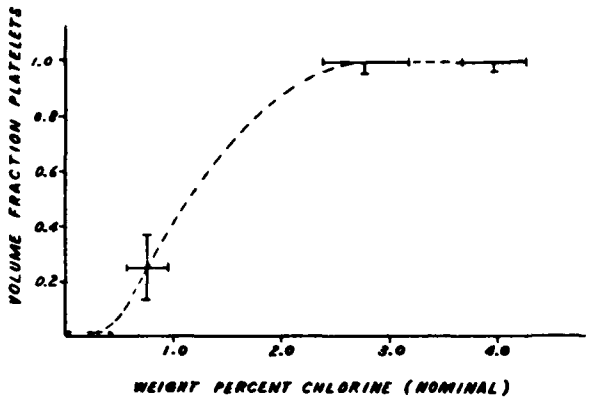

FIG. 5. Volume fraction of NaCl phase (platelets) retained after pressure quenching is plotted as a function of the nominal Cl content.

produced little effect on the grain size observed.

In the AI samples, both the retained NaCl phase (platelets) and wurtzite (and zinc-blende) matrix-phase grain size appeared bimodal, and had similar distributions. Both phases were composed of a mixture of equiaxed crystallites 10–50 μm in diameter and platelets 100–300 μm in diameter and 15–30 μm in thickness oriented roughly perpendicular to the load axis. Fast-quenched and slow-quenched samples were very similar in appearance.

The above results suggested an influence of the specimen composition on the postquench morphology. Microstructural investigation over a wide variation of Cl contents confirmed this suspicion. The volume fraction of NaCl phase (platelet) retained and the microstructural features observed seems to vary continuously with the Cl level of the starting material as shown in Fig. 5.

The internal structure of the NaCl phase (platelets) were studied using optical microscopy and surface-electron-microscopy (SEM) techniques. No discernable microstructure was observed in the platelets to within the resolution of these techniques. The platelets showed little optical rotation in polarized light and were harder than the polycrystalline matrix material. Transverse cracks were generally observed in the platelets which often terminated at the interface between the platelets and matrix material. The latter result is interpreted as evidence of the brittle nature of the platelets and results from the large volume change which occurs in the NaCl-to-wurtzite transition upon depressurization.

Although crystal structure determination of the platelets was not made directly on those samples having less than 20 vol % of platelets, it can be deduced that the platelets are of the retained NaCl high-pressure crystal structure. This deduction is based on the following facts: (i) The platelets of NaCl structure observed in samples highly doped with Cl, where the platelet volume fraction is greater than 90 vol %, were similar in character to the platelets observed in the lower-Cl-content material, and (ii) the qualitative estimate of the amount of quenched-in NaCl phase determined from ooth the DSC and x-ray measurements were in good agreement with the volume fraction of platelets determined in similar samples. Both sets of measurements correlated with the nominal Cl content.

VII. DISCUSSION OF EXPERIMENTAL RESULTS

Several interesting results are apparent from an examination of these data.

(i) The largest diamagnetism exceeded the largest paramagnetism observed by about an order of magnitude for the AI material containing 0.72 wt. % Cl.

(ii) The large scatter of susceptibilities observed for CdS materials having $0.7 < \mathrm{Cl} < 0.83$ wt. %. If one conservatively defines anomalous magnetic behavior when $\chi_{\text{sample}} > 10\chi_{\text{literature}}$, then the reproducibility of obtaining anomalous behavior was about 57% for this group. A somewhat lower "success" rate was obtained in sample material prepared by techniques described in this paper (about 35%) than in the as-received AI material.

(iii) Another rather subtle result is that, with the exception of a single sample of CdS containing 0.16 wt. % Cl, which was prepared by the acid-doping technique, all magnetically active samples were prepared by precipitation from an aqueous bath and had a nominal Cl content between 0.7 and 0.83 wt. %. (The role of Si in conjunction with Cl, if any, is not known at present.)

(iv) We have not observed lossless electrical conduction in any of our samples.

VIII. DISCUSSION

These results show that the conditions under which the anomalous electrical and magnetic behavior may occur are the rapid pressure quenching (greater than 10^5 bar/sec) from above the wurtzite-to-NaCl phase-transition pressure in CdS samples doped with Cl to levels in the range of 0.75 ± 0.1 wt. %.

The results also show that there is considerable scatter in the measured susceptibilities in this range. The many possible parameters that could generate this scatter are either uncontrollable or uncontrolled under present experimental conditions. The former category includes the possibility of critical ranges in the minor constituents of our material (~ 10 ppm) and quenching defects. The latter category includes the ambient conditions of the material-preparation process, chemical variability of the Cl impurity in samples prepared from the same lot, elapsed time between the pressure treatment and magnetic measurement, sample surface contamination with Si from the pyrophyllite gaskets (although the results of Nam *et al.*[2] would seem to obviate this possibility), etc.

The metastability of the measured susceptibilities[10,11] and their variability described above suggests that this anomalous behavior may be caused by some critical structural or chemical phenomena.

To examine the nature of such a critical phenomena, let us speculate on the interelationship of the quenching process and sample chemistry. The quenched-in platelets (presumably the retained NaCl phase) appear featureless under SEM examination to a resolution of about 10^4 Å.

The existence of these platelets are not the necessary and sufficient conditions for the anomalous behavior since they exist in samples which never showed the anomalous behavior and remain in samples in which the anomalous behavior has decayed to below the detection limits of the magnetometers. Also, we can accomplish nearly complete recovery of the NaCl phase in samples with a Cl content larger than 2.8 wt. % without pressure quenching. None of the latter samples together with fast-quenched samples from the same group ever showed detectable anomalous magnetic behavior.

We consider therefore a metastable decomposition of the high-pressure NaCl phase. This decomposition is strongly dependent on quenching statistics within a narrow range of sample chemistry. The metastability, as determined from electrical and magnetic measurements, has been shown to depend on annealing conditions.[11] We are unable to determine any structural change in the character of the platelets (NaCl phase) to the limit of the resolution of the SEM; thus such a decomposition may involve the motion of a mobile specie, e.g., Cl in interstitial sites.

Gibbs[18] separated into two categories the infinitesimal changes to which a metastable phase (e.g., NaCl phase) must be resistant. One is a change that is infinitesimal in degree but large in extent, as exemplified by a small compositional fluctuation spread over a large volume. Cahn[19] has shown that the early stages of such a decomposition (spinodal decomposition) in a solid proceed in a continuous and coherent manner such that detection is usually accomplished by observing the resultant periodic elastic strain effects on physical properties. To experimentally study such a process, one would require techniques sensitive to unusual electronic distribution and behavior, since we recognize that the anomalous effects reported here must ultimately be related to such electronic behavior, whatever the underlying physical structure.

Of course other models for such phenomena exist.[2-6] Only further experimental tests will determine which, if any, of these models apply or if a new collective phenomenon is occurring in these samples.

IX. CONCLUSION

The anomalous electrical and magnetic properties occur in CdS samples which have been heavily doped with Cl to levels of 0.75 ± 0.1 wt. % after pressure quenching from above the high-pressure phase transition at rates in excess of 10^5 bar/sec.

The material which may exhibit these anomalous phenomena can be prepared by precipitation from a Cl-containing bath if the resultant Cl concentration is within the range above.

The active material is not a simple mixture of CdS and $CdCl_2$, but rather a material containing (a) CdS_xCl_{1-x} complex(es). The particular complex(es) has (have) not been identified nor has (have) the structure(s) of the complex(es) been determined in the anomalous samples at present.

ACKNOWLEDGMENTS

We would like to acknowledge the following persons for their aid in performing this survey. Mrs. T. V. Brassard for metallographic preparation and L. McNamara for SEM analysis at Benet Weapons Laboratory, W. Koch for the chemical analysis, H. Parker for the solid-state sintering studies, F. Brinckman for suggesting the Cl-complex–formation analysis, R. Munro for calculating the species concentrations at NBS, and S. Bilodeau and K. Laojindanpun for their aid in performing the magnetic measurements at Rensselaer Polytechnic Institute (RPI). Support for this work is gratefully acknowledged and was supplied through the U.S. Air Force Office of Scientific Research Contract No. 79-0126 and under Contract No. N00014-80-C-0828 at RPI and additional grants from the U.S. Army Armament and Development Command Project No. 5004-07-001 at both RPI and NBS.

[1] E. Brown, C. G. Homan, and R. K. MacCrone, Phys. Rev. Lett. 45, 478 (1980).

[2] S. B. Nam, Physica 147B, 715 (1981); D. C. Reynolds, Y. Chung, and S. B. Nam, Air Force Weapons and Armament Laboratory Report No. AFWAL-TR-82-1031 (unpublished), available through National Technical Information Service Accession No. AD-A120 156/5.

[3] N. B. Brandt, S. V. Kuvshinnikov, A. P. Rusakov, and M. Semyonov, Zh. Eksp. Teor. Fiz. Pis'ma Red. 27, 37 (1978) [JETP Lett. 27, 37 (1978)]; C. W. Chu, A. P. Rusakov, S. Early, T. H. Geballe, and C. Y. Huang, Phys. Rev. B 18, 2116 (1978).

[4] T. H. Geballe and C. W. Chu, Commun. Solid State Phys. 9, 115 (1979); V. L. Ginzburg, Solid State Commun. 38, 991 (1981).

[5] S. B. Nam and D. W. Allender (private communication).

[6] T. C. Collins, M. Seel, J. J. Labik, M. Chandrasekhar, and H. R. Chandrasekhar, Phys. Rev. B 27, 140 (1983).

[7] R. K. MacCrone and C. G. Homan, Solid State Commun. 35, 615 (1980); C. G. Homan and R. K. MacCrone, J. Non-Cryst. Solids 40, 369 (1980).

[8] C. G. Homan, K. Laojindanpun, and R. K. MacCrone, Physica 107B, 9 (1981).

[9] C. G. Homan, K. Laojindanpun, and R. K. MacCrone, Solid State Commun. 45, 733 (1983).

[10] C. G. Homan, D. P. Kendall, and R. K. MacCrone, Solid State Commun. 32, 521 (1979).

[11] C. G. Homan and D. P. Kendall, Army Technical Report No. ARRLCB-TR-79004 (unpublished), available through NTIS, Springfield, VA, AD No. A069-609.

[12]G. A. Samara and H. G. Drickamer, J. Phys. Chem. Solids 23, 457 (1962).
[13]J. A. Small, D. E. Newbury, and R. L. Mylebust, in *Microbeam Analysis*, edited by D. E. Newbury (San Francisco University Press, San Francisco, 1979), p. 243.
[14]R. L. Mylebust, C. E. Fiori, and K. F. J. Heinrich, NBS Technical Note 1106, Frame C (1979) (unpublished).
[15]P. J. Cote, G. P. Capsimalis, and C. G. Homan, Appl. Phys. Lett. 38, 927 (1981).
[16]W. Koch, Anal. Chem. 54, 340 (1982).
[17]R. Sato and H. Itoh, Jpn. J. Appl. Phys. 3, 626 (1964).
[18]J. W. Gibbs, *Collected Works* (Yale University Press, New Haven, Conn., 1948), pp. 105–112 and 252–258.
[19]J. W. Cahn, Trans. AIME 242, 166 (1968).

END

FILMED

1-84

DTIC